A Variance-Based Sensitivity Analysis of a Goodwin-Keen type Economic Model

Pierre-Yves Longaretti, Hugo A. Martin

A Variance-Based Sensitivity Analysis of a Goodwin-Keen type Economic Model*

Pierre-Yves Longaretti† and Hugo A. Martin‡

Abstract.

Sensitivity analysis is a well-known tool of the trade in a number of scientific fields, but is not yet widespread in economics, in spite of its central usefulness in evaluating a model robustness. Furthermore, the discipline makes scant use of dynamical modeling, to the notable exceptions of the post-keynesian and ecological economics sub-fields, where a rigorous and versatile macroeconomic dynamical modeling framework, dubbed *stock-flow consistent* (or SFC) modeling, is gaining popularity.

The purpose of the present paper is to present a two-tiers form of variance-based sensitivity analysis, focusing first on parameter groups before looking at individual parameters themselves in the context of macroeconomic dynamics. Such an approach offers a powerful way to tackle models with moderate to large numbers of parameters in a hierarchical fashion, helping researchers to make sense of the results of a sensitivity analysis and of its insight into their model dynamics. We deploy this method on a recent model (IDEE) in the Goodwin-Keen family, as the Goodwin-Keen approach to nonlinear macroeconomic dynamics has gained a lot of momentum in the last two decades. IDEE is a model of intermediate complexity; as many similar models, its macroeconomic core harbors highly nonlinear interrelationships among key economic variables such as employment rate, wage share, debt ratio, and inflation rate.

Our findings highlight the paramount influence of parameter groups dictating shareholders' incomes in shaping value distribution within the model. Interestingly, while inflation has historically been considered pivotal in prior studies, our analysis suggests that it plays a relatively minor role in trajectories converging toward a Solow-type attractor—except insofar as it influences bifurcating dynamics. Finally, and perhaps most importantly, the sensitivity analysis performed allows us to show that the model results are robust with respect to expected variations and uncertainties in its parameters' values. We believe that the numerical methods presented in this paper can help to understand and improve numerical economic models, and eventually to improve their overall soundness and robustness.

Key words. Goodwin-Keen model, variance-based sensitivity analysis, stock-flow consistency

MSC codes. 34C60, 91B55, 91B82

1. Introduction.

Sensitivity analysis methods are essential tools in various scientific fields (such as economics, engineering, environmental science, and finance) for understanding how variations in model inputs affect outputs. These techniques [46, 38, 10, 51, 3, 47, 35, 40] help identify which parameters have the most significant impact on the model's behavior and can also highlight the robustness and reliability of a model. It is particularly useful in scenarios where models are complex, and computational resources are limited. Overall, sensitivity analysis enhances the interpretability of models, supports model validation, and contributes to the development of more resilient and efficient systems. Among the various sensitivity

*This file was written using the SIAM online LaTeX template.

Funding: This work was funded by the French National Institute on Digital technology (INRIA) through its "Action Exploratoire" on global systemic risks AEX RSG.

†Équipe-projet STEEP, Laboratoire Jean Kuntzmann (LJK), CNRS, GINP, INRIA, Unversité Grenoble Alpes, Montbonnot-Saint-Martin, 38330, FRANCE

‡Équipe-projet STEEP, Laboratoire Jean Kuntzmann (LJK), CNRS, GINP, INRIA, Unversité Grenoble Alpes, Montbonnot-Saint-Martin, 38330, FRANCE; and Environmental Justice Program, Georgetown University, Washington, DC, 20057, USA. (martin_hugo@ymail.com),

analysis techniques, Sobol methods [46, 43, 44] are widely used for their ability to quantify the contribution of both individual parameters and interactions between parameters (or groups of parameters), making them particularly valuable for analyzing complex, non-linear models.

In the field of Ecological Economics, mathematical models and numerical simulations serve as a means of anticipating the effects of our economic policies on both the economy and the environment to address the crucial challenges of overcoming the losses caused by climate-related damages[30, 31] and managing the additional costs of mitigation activities[8, 45, 50, 31, 48]. These models must therefore incorporate climate dynamics coupled with economic dynamics. Within the family stock-flow consistent (SFC) models [18], whose economic dynamics are inherently out of equilibrium and governed by non-linear differential equations, such models have been coupled with climate models of varying complexity [11, 4, 12, 33, 37]. The advantage of these models is that they do not require assuming gross domestic product (GDP) growth over the short, medium, or long term, nor do they assume equilibrium will be achieved a priori—contrarily to equilibrium models like the Dynamic Integrated Climate-Economy (DICE) model [39] and its successive variants [25]. Nevertheless, such equilibria (attractor points in the system's phase space) may exist and be reached. Trajectories then typically exhibit business cycles (oscillations) [19, 1, 53, 34], whose characteristics (amplitude, frequencies) are determined by the parameters' values.

However, the non-linear nature of differential equations presents challenges in the parameterization of SFC models and their computational code [2]. It can be difficult for the modeler to ensure the robustness of numerical simulation results when assigning values to the model's parameters. In what follows, we will distinguish between the parameters corresponding to the initial conditions and the parameters of the various equations in the model (referred to as model parameters). Given initial conditions and a set of parameters, it is desirable that a small modification of a model parameter does not radically alter the simulated trajectory. Mathematically, we want to avoid placing the system at the boundary of an attraction basin with the chosen initial conditions and parameter set, and be aware of any critical parameter that could drastically change the simulation trajectories if modified. More often than not, the ambiguity lies in the values of the model parameters rather than the initial conditions, which is constrained by econometric studies and real data. A sensitivity analysis of the variations in output quantities as a function of input parameters can then help resolve such ambiguities, while maintaining the model within acceptable parameter limits from an economic point of view.

In this paper, we present a Sobol varianced-based sensitivity analysis of the computational code of the Integrated Dynamic Environmental Economics (IDEE) model, which is based on the model developed in Martin et al. (2023) [37], which itself builds on the Bovari et al. (2018) [4] model and its variants [7, 6, 5]. IDEE is based on a macroeconomic model coupled with an Earth Model of Intermediate Complexity (EMIC) called *i*LOVECLIM [41], which includes a physical representation of the atmosphere, ocean, sea-ice, and vegetation. The IDEE model then is a coupled climate/SFC model and has at least two stable equilibrium points: a "good" (Solow type) equilibrium, where the economy maintains a controlled employment rate and private debt, and a "bad" equilibrium where the economy collapses, with the employment rate converging to zero and private debt skyrocketing. Preliminary sensitivity analyses of earlier versions of the IDEE code have been conducted in Bovari et al. (2018) [4, 7], with a

more advanced analysis presented in Bolker et al. (2021) [2].

More specifically, Bovari et al. (2018) [4] explores, for an earlier version of the model, the attraction basins (i.e., varying initial conditions) of the "good" attractor for a given set of parameters (see their figure 3), and examines the influence of carbon prices (figure 8) as well as of damage functions (figure 9) on trajectories. In Bovari et al. (2018b) [7], the authors employ a Monte Carlo method to study uncertainties, specifically the effects of the model productivity growth rate, equilibrium climate sensitivity, and carbon absorption on the outcome of the simulation in 2100 (figure 3), private debt levels in 2100 (figure 4), and temperature anomalies in 2100 (figure 5). However, this study does not quantify the influence of individual parameters on model outputs or their interactions. By conducting 1 000 simulations, Bolker et al. (2021) [2] expanded these results with a sensitivity analysis of parameters modeling price adjustment speeds, firms' markup prices, and the degree of money illusion in the conflict over value-added distribution. In particular, they show that the influence of the price markup parameter is critical and of primary importance, as it drastically alters the model's attraction basins (see Bolker's figure 2). Bolker's study is noteworthy for quantifying logistic regression coefficients and partial rank correlations (figure 3). To our opinion, its limitation, however, is that it focuses only on results presented in 2100 and does not address the timescale of the model's asymptotic convergence to its attractors. Furthermore, the maximum sample size of simulations in their study is 1 000, which is relatively adequate for such a limited study but is much too small for an exhaustive analysis, given the number of parameters (about 20 parameters for the economic side of IDEE, not including the initial conditions).

The economy/climate relationships in this model have been thoroughly examined; see, e.g., [4, 37]. Consequently, the present paper focuses on the purely economic aspect of the IDEE model through a sensitivity analysis of its 19 parameters, involving over 240 000 simulations. We analyze the influence of the variance of these 19 parameters on the variance of 14 output quantities, including novel metrics such as the frequency and amplitude of business cycles and the relaxation time toward a stable equilibrium. For each output quantity, we define a ranking index which orders the parameters in decreasing influence in the variations of the output. Next we quantify the robustness of this parameter ranking through two novel robustness criteria. The first quantifies the robustness of the ranking between a pair of parameters relative to each other, while the second quantifies the robustness of the overall ranking of all parameters simultaneously.

This paper is organized as follows. We first briefly recall the IDEE model equations and properties in section 2. Section 3 outlines the principles of the variance-based sensitivity analysis method we employed and describes how the different output quantities were defined and calculated. Section 4 presents the results of the sensitivity analysis of the IDEE model, first for groups of model parameter and then for the individual parameters of the most significant groups. We revisit the criticality of the price markup highlighted by Bolker et al. (2021) [2] in section 5. Finally, we present a few computational aspects of our study in section 6.

Although we use IDEE as a case study for this analysis, we echo the point made in Bolker et al. (2021) [2]: uncertainty must be addressed for all dynamical models through sensitivity analysis. This point is crucial, as it would both highlight unexpected behaviors in SFC models that may be difficult to anticipate analytically and validate the computational implementations of SFC models, thereby enhancing the robustness of numerical results. To

inspire economic modelers to adopt such methods, we are making the sensitivity analysis code we used available open-source on GitHub [29].

2. IDEE model. To assess the macroeconomic impact of climate change and policies, we use model IDEE introduced in Martin et al. (2023) [37]. This idealized economy is divided into households, firms, the public sector, and banks. The relative simplicity of this model enables the identification of some of its mathematical properties [4, 6, 5, 23, 22, 16, 21, 24, 17, 37].

There are typically two types of attractors. The first is a "good" Solow-type equilibrium, where employment rate, nominal wage rate, and the inverse of the private debt ratio simultaneously converge to non-zero, finite limits, while the economy follows a balanced growth path asymptotically. A catastrophic outcome occurs when climatic damages drive the economy out of the basin of attraction of this desirable equilibrium, ultimately pushing it into the basin of attraction of a second "collapse" attractor. This alternative long-term debt-deflationary equilibrium sees these same variables converge to zero, representing a catastrophic endgame for the economy [4].

In this framework, the dynamic interaction between Earth's climate and the global economy operates as follows. Each year, IDEE's climate component (*i*LOVECLIM) computes the annual mean climate state, based on the atmospheric greenhouse gas (GHG) concentration level. This climate state can cause economic damage, affecting production, capital, and economic growth. Consequently, global warming not only reduces total production, but also damages existing capital, impacting future production capacity.

To address these damages, the public sector can impose a carbon tax to incentivize firms' mitigation efforts. It can also provide subsidies to environmentally responsible companies through additional public expenditures. Meanwhile, the private sector may engage in abatement and repair activities to replace "dirty" or deteriorating infrastructure with cleaner alternatives. These interactions result in new GHG emissions, which are added to *i*LOVECLIM, ultimately producing a new climatic state.

2.1. Economic macro-dynamics. The economic component of IDEE includes 10 variables and related differential equations, divided into seven purely economic ones (workforce, labor productivity, total capital, total private debt, mean wage, inflation rate, short-term interest rate) and three related to technology and pricing for climate adaptation and mitigation (emission intensity of capital, carbon price, and price of green technology). Although all equations are presented below, as mentioned in the Introduction, the sensitivity analysis in section 4 focuses on the seven purely economic variables. Note that Table 2 from Appendix A presents all the model variables and parameters.

2.1.1. Workforce dynamics. The global workforce $N > 0$ is modeled to grow following a sigmoid function derived from the 15–64 age group in the U.N. median fertility scenario [13]

$$\dot{N} \coloneqq \delta_N N \left(1 - \frac{N}{\overline{N}}\right), \tag{2.1}$$

where $\overline{N} > 0$ represents the upper limit of the global workforce, and $\delta_N > 0$ determines the convergence speed. Based on our calibration, aligned with the U.N. median scenario, this plateau is expected to be reached shortly before 2100.

2.1.2. Labor productivity dynamics. Labor productivity $a > 0$ is modeled to grow at an endogenous rate:

$$\frac{\dot{a}}{a} \coloneqq \max\left(\delta_a^{\min}, \delta_a + \gamma_g g\right), \tag{2.2}$$

where $\delta_a^{\min}$ is constant, δ_a is the intercept and $\gamma_g \geq 0$ is the slope, and g represents the real growth rate of the global economy. Equation (2.2) is based on the Kaldor-Verdoorn stylized model of endogenous growth [15]. It introduces hysteresis, i.e., path-dependence, into the overall economic dynamics [17]. The resulting economy retains both a Solovian equilibrium and a catastrophic one; see Figures 1 and SM1 in Supplementary Materials.

To define g, we need to introduce the production function. In the absence of climate change, firms can produce a potential real output $Y^0 > 0$, of a single, synthetic consumption good by combining the available workforce N and capital K—whose dynamics are given by (2.1) and (2.5), respectively—as complementary factors of production, i.e.,

$$Y^0 \coloneqq \min\left\{\frac{K}{\nu}; aN\right\}, \tag{2.3}$$

where $\nu > 0$ represent (constant) capital-to-output ratio. The constancy of the capital-output ratio aligns with most of the post-Keynesian literature on ecological macroeconomics [26].

Economic activities generate greenhouse gas (GHG) emissions, which are subject to a carbon tax imposed by the public sector. To reduce the tax burden, firms may engage in abatement activities, resulting in a fraction of the output Y^0—denoted A—being diverted from the commodity market and used as intermediate consumption to mitigate emissions. This abatement implies that part of the labor funded by firms does not generate immediate private profit. Instead, this labor may be involved in R&D sectors, which, while not directly profitable, accelerate the transition to a more sustainable industry.

Furthermore, as in DICE [39], a proportion D_Y of the remaining production is lost due to global warming. Thus, the final production level is:

$$Y \coloneqq (1 - \delta_Y)Y^0, \tag{2.4}$$

with $\delta_Y \coloneqq 1 - (1 - D_Y)(1 - A)$, allowing us to calculate $g \coloneqq \dot{Y}/Y$. Both quantities D_Y and A are precisely defined in subsections 2.2 and 2.3.2.

2.1.3. Capital accumulation dynamics. The total capital stock is represented by $K > 0$, with the capital accumulation equation given by:

$$\dot{K} = I - (\delta_K + \Gamma)\, K, \tag{2.5}$$

where I, δ_K, and $\Gamma \geq 0$ are non-negative quantities that represent respectively the real investment in capital, the capital depreciation rate, and the fraction of capital seized by the banking sector when owners default on their corporate debt.

Real capital depreciation is expressed as $\delta_K K$. The depreciation rate δ_K is defined as $\delta_K \coloneqq \delta + D_K$, where $\delta > 0$ is the constant standard depreciation rate, and D_K is the rate of capital depreciated due to climate change; see details in subsection 2.2. Note that the

term $\delta_K K$ can be interpreted as a forced investment (firms invest at least to compensate for depreciation). Consequently, it appears in the model equations wherever investment I is present to ensure stock-flow consistency.

Regarding investment I, it is driven by the return rate on capital $\pi_K \coloneqq \Pi/pK$—where p represents the price (with its dynamics governed by (2.13))—which reflects the productive sector's risk appetite. To proceed, we define the firms' nominal profit Π before dividends, calculated as the nominal output pY *minus* production costs:

$$\Pi \coloneqq pY - W - p\delta_K K - rD - pT_f, \tag{2.6}$$

where the total cost components are: (i) the money wage bill $W \geq 0$; (ii) the nominal capital depreciation $p\delta_K K \geq 0$; (iii) the debt service repayment rD—with D the total nominal debt of firms (whose dynamics are detailed in (2.10)), and $r \geq 0$ being the short-run nominal interest rate firms pay to the banking sector ((2.14))—and (iv) the carbon tax $pT_f \geq 0$, defined in subsection 2.3.2.

The money wage bill $W \coloneqq wL$ is determined by the mean wage $w \geq 0$ ((2.11)) and the number of active workers $L \geq 0$. Depending on the available capital, firms minimize costs by employing the required amount of labor L to utilize capital at full capacity, i.e., (2.3) provides $L \coloneqq Y^0/a = K/(\nu a)$.

Investment is then defined by:

$$I = \kappa(\pi_K) Y \left(1 - \frac{(1-\delta_Y)d}{\nu}\right)^{\zeta_I}, \tag{2.7}$$

with $\zeta_I \geq 0$ and where $\kappa(.)$ is an increasing linear function (with κ_0 as the intercept and κ_1 as the slope) taking values in $[0;1]$ and $d \in [0;1]$ is the private debt ratio, i.e.,

$$d \coloneqq D/pY. \tag{2.8}$$

Turning to Γ that appears in (2.5), the fraction of capital seized by the banking sector, current profits may not be sufficient to cover the entire investment I, necessitating firms to borrow from the banking sector. However, like much lending in modern economies, corporate debt is collateralized by the current stock of capital, valued at its market price pK [37]. As a proxy, it is assumed that the productive sector ceases to invest whenever the total debt D gets close to the total capital pK, i.e., when d converges to $\nu/(1-\delta_Y)$.

Consequently, default leads to a transfer of ownership over the collateral from borrowers to lenders. It is then modeled such that, given a debt ratio d, the fration $\Gamma \in [0,1]$ is defined as:

$$\Gamma \coloneqq 1 - \exp\left(-\frac{\chi\left((1-\delta_Y)d\right)^2}{\nu^2 - \left((1-\delta_Y)d\right)^2}\right), \tag{2.9}$$

indicating the ratio of capital seized by the banking sector and thus no longer operational. For sufficiently large $\chi > 0$, Γ effectively converges quickly from 0 to 1 when d gets close to $\nu/(1-\delta_Y)$. As a result, the private debt ratio is endogenously capped.

2.1.4. Private debt dynamics. The evolution of nominal private debt D is described by the equation:

$$\dot{D} = pI - \Pi_r - p\left(\delta_K + \gamma_\Gamma \Gamma\right) K, \tag{2.10}$$

where all the terms are variables except for the constant $\gamma_\Gamma \geq 0$ that represents a kind of "debt forgiveness ratio". It means that a slightly higher portion than the capital seized of the aggregate debt is removed when the latter is close to the level $\nu/(1-\delta_Y)$ (see subsection 2.1.3), providing the economy with some breathing room when the situation becomes highly critical. Π_r denotes firms' nominal profit after dividend payments to shareholders from Π.

More specifically, a fraction $\Delta(\pi_K) \in (0,1)$—typically modeled as an increasing linear function with intercept Δ_0 and slope Δ_1—of nominal output is distributed to households as dividends, provided that the profit before dividends Π is non-negative. Consequently, the retained earnings of the corporate sector Π_r are defined as $\Pi_r = \Pi - \Pi_f$, where $\Pi_f \coloneqq \Delta(\pi_K) pY$ if $\Pi > 0$, and $\Pi_f = 0$ otherwise.

2.1.5. Mean Wages dynamics. The primary link between the real and nominal spheres of the economy [21] is modeled through a short-run Phillips curve [20, 36], which connects the growth rate of nominal wages *per-capita* w to the employment rate λ [4, 5] via the following equation:

$$\frac{\dot{w}}{w} \coloneqq \sqrt{1-\omega}\left(\varphi(\lambda) + \gamma_w i\right), \tag{2.11}$$

where $\omega \in [0;1]$ is the wage share, $\varphi(\cdot)$ is an increasing linear function taking values in $[0;1]$ (with intercept ϕ_0 and slope $\phi_1 \geq 0$), $\lambda \in [0;1]$ is the employment ratio, $\gamma_w \geq 0$ measures the degree of money illusion [2], and i is the inflation rate of price p; see (2.13).

The wage share and the employment ratio are defined by

$$\omega \coloneqq \frac{wL}{pY} \qquad \text{and} \qquad \lambda \coloneqq \frac{L}{N}. \tag{2.12}$$

Note that the factor $\sqrt{1-\omega}$ in (2.11) simply ensures that the wage share ω cannot exceed 1.

2.1.6. Price of goods dynamics. The second (and final) link between the real and nominal sectors [23] involves the price of goods, $p \geq 0$. The dynamics of the price inflation rate i emerge from the adjustment of current prices at a rate $\eta > 0$ towards their endogenous long-run value:

$$i \coloneqq \frac{\dot{p}}{p} \coloneqq \eta\left(\mu\omega - 1\right), \tag{2.13}$$

where μ is a price "markup", and ω still denotes the wage share. Strictly speaking this quantity is not exactly the markup defined as the difference between the unit price and unit production cost; in this case, the right-hand side should read $\eta\left(\mu\omega - C\right)$ where C is a constant. However, one may easily eliminate this extra constant by rescaling μ and η accordingly. As μ is never actually used here according to its exact definition just stated, this has no impact on the dynamics and eliminates one constant from the problem.

In IDEE, μ is endogenously determined as a function of the return on capital: $\mu \coloneqq \max\left(1, \mu_0 + \pi_K\right)$, where $\mu_0 \geq 1$. In essence, the market power of firms—as reflected by the markup—is modeled as an increasing, linear function of the return on capital.

2.1.7. Short-term interest rate dynamics. The short-term interest rate $r \geq 0$ is modeled to follow a standard Taylor rule [52]:

$$\dot{r} = \eta_r \left(r_{CB} - r\right), \tag{2.14}$$

where r_{CB} represents the Central Bank interest rate and $\eta_r > 0$ is a relaxation parameter that determines the adjustment speed of the interest rate.

The Central Bank interest rate $r_{CB} \geq 0$, is defined as $r_{CB} \coloneqq \max\{0; r^* + i + \psi(i - i^*)\}$, where $r^* \geq 0$ represents the long-term real interest rate targeted by the central banking system. The term i^* is the inflation rate typically targeted by the monetary policy authority, and $\psi > 0$ is a parameter that governs the extent of the central bank's response to deviations in inflation from its target.

2.2. Climate-related dynamics and Damage function. Every year, IDEE's climate component (the earth model of intermediate complexity *i*LOVECLIM) computes the annual mean climate state based on the atmospheric greenhouse gas (GHG) concentration level; see the details in [37]. This level evolves due to industrial emissions E_{ind} related to economic activities (see (2.16) in the next section. The global warming induces damages on production Y and capital K. The functional form and calibration of the damage functions are derived from Dietz and Stern (2015) [14]. Let ΔT denote the mean air temperature elevation. The damage function is defined as

$$\text{Dam} = 1 - \frac{1}{1 + \Upsilon_1 \Delta T + \Upsilon_2 \Delta T^2 + \Upsilon_3 \Delta T^{\zeta_3}}, \tag{2.15}$$

where $\Upsilon_1, \Upsilon_2, \Upsilon_3$ are positive scalars, and ζ_3 is a positive exponent. A fraction D_K of Dam impacts the capital by increasing its depreciation rate, which is expressed as $\delta_{D_K} \coloneqq \delta + D_K$, while D_Y affects the total output Y^0 (as in (2.4)), the damages D_K and D_Y being defined by $D_K \coloneqq f_K \text{Dam}$, and $D_Y \coloneqq 1 - (1 - \text{Dam})/(1 - D_K)$, where $f_K \in [0, 1]$ represents the fraction of damage attributed to the capital stock.

2.3. Abatement-related dynamics. To complete the system, we need to define two last quantities: the abatement ratio A, and the carbon tax T_f. This can be done by introducing three additional differential equations that govern the emission intensity of capital σ, the price of green (or backstop) technology p_{BS}, and the carbon price p_C.

2.3.1. Emission intensity dynamics. Depending on the carbon price level $p_C \geq 0$ (2015 USD per tCO_2e), firms endogenously select their emission reduction fraction $n \in [0; 1]$. Economic activities emit GHG emissions (tCO_2e), which are proportional to the total production Y^0 and are given by:

$$E_{ind} \coloneqq \sigma(1 - n)Y^0, \tag{2.16}$$

where $\sigma > 0$ represents the carbon-emission intensity of the economy. This intensity follows a semi-endogenous sigmoid function of time, governed by:

$$\frac{\dot{\sigma}}{\sigma} \coloneqq \delta_\sigma - \gamma_\sigma A, \tag{2.17}$$

where $\delta_\sigma \leq 0$ and $\gamma_\sigma \geq 0$, are a given parameters, and A is the abatement ratio, defined later in subsection 2.3.2, which accelerates the reduction of emission intensity toward greener technology as described by (2.17).

2.3.2. Green technology price dynamics. As in the DICE model [39], the abatement technology $A \geq 0$ is assumed to be a convex function of the emission reduction ratio, normalized by the emission intensity of the economy σ and the semi-endogenous price of a backstop technology $p_{BS} \geq 0$ (2015 USD per tCO_2e). Specifically, A is given by $A = \sigma p_{BS} n^\theta/\theta$, where $\theta > 0$ controls the convexity of the cost. The backstop technology price p_{BS} decreases at a constant (negative) rate $\delta_{p_{BS}}$ following the equation:

$$\frac{\dot{p_{BS}}}{p_{BS}} := \delta_{p_{BS}} - \gamma_{p_{BS}} A, \tag{2.18}$$

where $\delta_{p_{BS}} \leq 0$, $\gamma_{p_{BS}} \geq 0$. Here, n represents the fraction of production processes that are "de-polluted;" see (2.19). Note that, similar to the evolution of the emission intensity, the abatement activity A facilitates a faster decline in the backstop technology price p_{BS}.

Regarding the public sector, the primary instrument to promote the transition towards a zero-carbon economy is the carbon tax $T_f := p_C E_{ind}$, which is imposed on GHG emissions E_{ind}. A fraction s_A of the abatement costs incurred by firms is subsidized by the public sector, leading to a total transfer of $S_f = s_A A Y^0$, resulting in net transfers from the public to the private sector amounting to $S_f - T_f$.

In response to the policy set by the public sector, firms determine the emission reduction ratio, n, that minimizes the sum of abatement costs and carbon tax, expressed as $\min_{n\in[0,1]} AY^0 + T_f - S_f$. Thus, the optimal aggregate abatement fraction of GHG emissions is:

$$n = \min\left\{\left(\frac{p_C}{(1-s_A)p_{BS}}\right)^{1/(\theta-1)}; 1\right\}. \tag{2.19}$$

2.3.3. Carbon price dynamics. The public sector's influence is encapsulated in two variables (p_C and r_{CB}), and one parameter s_A, which represents the fraction of public subsidies. Both variables impact the profit share, thus influencing the overall macro-dynamics through investment flows. The implementation of policy scenarios is greatly facilitated by assuming that the carbon price is assumed to follow an exogenous trajectory as outlined by the Report of the High-level Commission on Carbon Prices [49]. The real carbon price $p_C \geq 0$ is modeled to grow exogenously at a specified rate, based on a simple parametric carbon price function:

$$\frac{\dot{p_C}}{p_C} := a_{p_C} + \frac{b_{p_C}}{t}, \tag{2.20}$$

where $a_{p_C} \geq 0$ denotes the long-term growth rate trend of the carbon price, and $b_{p_C}/t \geq 0$ captures the time-varying component of the growth rate, with t representing the number of years since the policy's inception.

2.4. Reduced IDEE Model. As mentioned in the Introduction, the sensitivity analysis conducted in this article focuses on the economic aspect of the IDEE model. Therefore, in section 4, we assume no climate damages, i.e., $\Delta T = 0$ in (2.4), leading to Dam $= 0$ and $D_Y = D_K = 0$. Consequently, we also set the carbon price to zero, meaning $a_{p_C} = b_{p_C} = 0$ in (2.20), resulting in $p_C = n = 0$ and $A = 0$.

These assumptions imply that $\delta_Y = 0$ in (2.4), leading to $Y = Y^0$, and leaving the three differential equations (2.17) (2.18) and (2.20) without any influence on the trajectories of the other variables.

This allows us to disregard them, resulting in a reduced form of IDEE derived from the 7 differential equations presented in subsection 2.1. This reduced model now consists of 5 differential equations (2.21)-(2.25), involving the following variables: the debt ratio d, the wage share rate ω, the employment rate λ, the workforce N, and the interest rate r; involving 3 quantities (2.26)-(2.28): the inflation rate i, the real growth rate g, and the return on capital π_K. One has:

$$\dot{d} = d\left(r - i - g\right) - \left(1 - \omega\right) + \Delta\left(\pi_K\right) + \left(g + \delta\right), \tag{2.21}$$

$$\frac{\dot{\omega}}{\omega} = \sqrt{1-\omega}\left(\varphi\left(\lambda\right) + \gamma_w i\right) - \delta_a - \gamma_g g - i, \tag{2.22}$$

$$\frac{\dot{\lambda}}{\lambda} = \left(1 - \gamma_g\right) g - \delta_a - \frac{\dot{N}}{N}, \tag{2.23}$$

$$\frac{\dot{N}}{N} = \delta_N \left(1 - \frac{N}{N^\star}\right), \tag{2.24}$$

$$\dot{r} = \frac{1}{\eta_r}\left(r^\star + i + \psi\left(i - i^\star\right) - r\right), \tag{2.25}$$

with

$$i = \eta\left(\left(\mu_0 + \pi_K\right)\omega - 1\right), \tag{2.26}$$

$$g = \frac{\kappa\left(\pi_K\right)}{\nu}\left(1 - \frac{d}{\nu}\right)^{1/4} - \delta, \tag{2.27}$$

$$\pi_K = \frac{1}{\nu}\left(1 - \omega - rd - \nu\delta\right). \tag{2.28}$$

This model form particularly highlights that the variables d, ω, and λ involve multiple complex non-linear interactions with various other variables.

The dynamics governed by the model (2.21)-(2.28) are the focus of the sensitivity analysis presented in section 4. However, it is important to note that the computational code of IDEE—the actual object analyzed in this article—is based on a time discretization of the 10 differential equations previously introduced in subsections 2.1 and 2.3. For more details on the computational aspects, see section 6.

3. Method: Variance-based Sensitivity Analysis.

3.1. Pre-analysis. The sensitivity analysis we conduct involves varying a set of input parameters within predefined intervals and studying how these variations impact the output

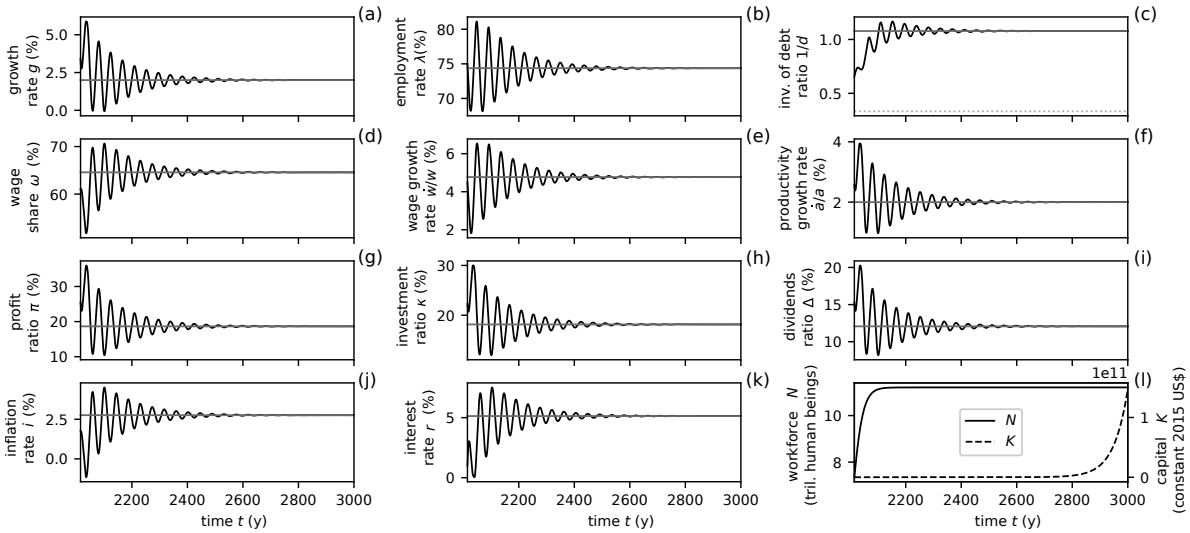

Figure 1. *Trajectories of the output quantities under the scenario computed with the default parameter values. The horizontal gray lines represent the values around which the oscillations average over the last simulated century. These average values (represented in figures (a)-(i)), toward which the trajectories converge, are 11 of the 14 output quantities whose variations are analyzed in the sensitivity analysis.*

quantities. We begin this section by presenting the selected output quantities, followed by the input parameters and their range of variation.

Figure 1 represents a typical trajectory obtained using the default parameter values that we specify in Tables 3 and 4; see Appendix A. This trajectory is a reference trajectory chosen for its plausibility and for its oscillating and converging behavior, which could not be achieved if the model were parameterized using econometric data-based values. We did not specifically aim to calibrate these trajectories given the asymptotic study we are conducting here. The end year of the simulation (3000) is not chosen for realism but in order to check numerically the model convergence on the point of attraction in the absence of economic and political perturbations or disruptions (here, the Solow-like balanced growth point, i.e., the model "good" attractor), given the oscillation time scale (~ 50 y) and the damping time scale ($\sim 100 - 200$ y). These oscillations are due to the wage/employment dynamics driven by the Phillips curve; this is but one of the many possible causes of long term economic cycles. This also illustrates that typical initial conditions do not lead to a stationary growth model.

Figure 1 depicts 12 output quantities (see their descriptions in the figure's caption), including the three main variables of the reduced model: employment rate λ (b), private debt rate d (c), and wage share ω (d). For each of the Figure 1(a)-(k), the horizontal gray lines represent the average value of the trajectory over the last simulated century (i.e., the quantity ω_∞ shown in Figure 2(a) for the wage share). The population trajectory N is shown in Figure 1(l) as well as the total amount of capital K (the latter is shown here only for information but is not considered in the sensitivity analysis).

In the present article, we do not aim to analyze the role of the model initial conditions,

as their values are relatively well constrained by econometric data. In this article, our focus is solely on varying the model parameters. We also aim to vary these parameters in such a way that the variations in output quantities remain relatively limited. For example, we are not seeking to shift trajectories towards the "bad" attractor as in Bolker et al. (2021) [2], but rather to explore variations around the "good" attractor. This includes studying the relaxation time towards the latter point and the amplitude of oscillations around it.

Figure 2 illustrates a temporal trajectory of the wage share ω over a very long simulated time period (from 2015 to 3000). Additionally, it provides a graphical representation of several selected output quantities. The variations of these quantities will be studied in relation to changes in parameters in the sensitivity analysis. For instance, the quantity ω_∞ represents the average value of the wage share at the end of the simulated time (from 2900 to 3000). The quantity C represents the degree of convergence toward the asymptotic limits, measured as the average amplitude of oscillations in the trajectory from 2600 to 3000. The main frequency of these oscillations is given by the quantity Ω (computed over the two first centuries). The relaxation time of the trajectory toward its average value is given by the quantity t_r, which is calculated as the minimum relaxation times t_{inf} and t_{sup} determined by the lower and upper envelopes of the trajectory. These envelopes are depicted by the dashed curves in Figure 2(a, b). These relaxation times are calculated from the steepest lower and upper tangents (α_{inf} and α_{sup}) shown in Figure 2(b). Note that the relaxation time t_r is calculated exclusively based on the wage share trajectory.

In our sensitivity analysis, we consider the variations of 14 output quantities, divided into 11 average values computed over the last century of the simulation (the growth rate g_∞, employment rate λ_∞, debt ratio d_∞, wage share ω_∞, wage growth rate $(\dot{w}/w)_\infty$, productivity growth rate $(\dot{a}/a)_\infty$, profit ratio π_∞, investment ratio κ_∞, dividends ratio Δ_∞, inflation rate i_∞, and interest rate r_∞), as well as the oscillation amplitude ratio C, the main frequency of the oscillations Ω, and the relaxation time t_r.

Now that the output values have been defined, we address the input parameters. We consider 19 parameters, which we subdivide into 8 groups (capital K, inflation i, investment I, productivity p, dividends D, population N, Phillips curve P, and interest rate r). To determine the intervals within which each parameter will take its values, we estimate their variation based on the functions in which they are involved. For example, the growth rate of labor productivity $\dot{a}/a$ is given by the equation:

$$\frac{\dot{a}}{a} = \delta_a + \gamma_g g, \tag{3.1}$$

where δ_a and γ_g are parameters and g is a variable representing the real GDP growth rate. Thus, by assuming a plausible trajectory for g (e.g., fluctuating around 2% annually), we can determine the intervals for the parameters δ_a and γ_w such that we control the induced variation in $\dot{a}/a$ (e.g., also around 2%). This example is illustrated in Figure 3(a)-(c). Figure 3(a) shows the set of labor productivity growth rates trajectories induced by different parameter values as a function of a plausible real GDP growth rate trajectory. Figure 3(b) displays the same set of productivity trajectories over time, and Figure 3(c) depicts a typical trajectory for the growth rate g used to determine Figure 3(a, b) from (3.1).

The lower and upper bounds of the parameter value intervals (the inputs δ_a and γ_g) are set

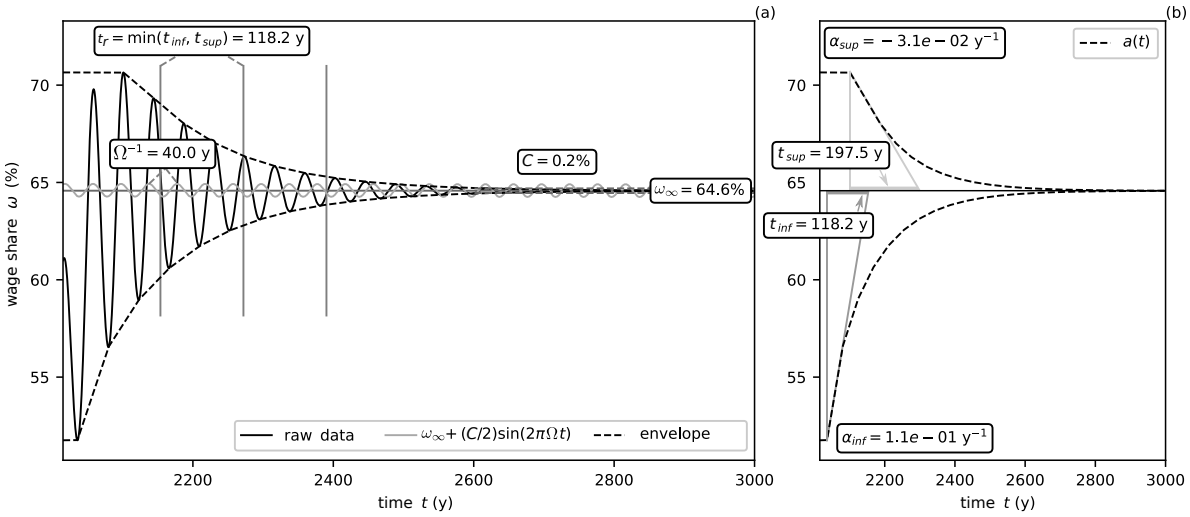

Figure 2. *Example of the wage share trajectory ω from which three output quantities in the sensitivity analysis are computed: the amplitude C of the oscillations between 2600 and 3000 around the average value ω_∞, the main frequency of the oscillations Ω (computed over the first two centuries), and the relaxation time t_r of the trajectory toward the convergence value ω_∞. The time t_r is taken as the minimum between the lower and upper relaxation times (t_{inf} and t_{sup}), which are themselves obtained from the steepest slopes (α_{inf} and α_{sup}) of the lower and upper envelopes (dashed curves around the trajectory).*

to obtain a pre-determined range of values for the productivity growth rate $\dot{a}/a$ (the output) at the end of the simulation. This range is centered around the value taken by the variable with the default parameter values (the red trajectory in Figure 3(a)-(b)). The output value interval fluctuates 50% below and above this average value; see Figure 3(b).

Similarly, Figure 3(d)-(f) provide an idea of the range of trajectories that the central bank interest rate can take based on the values of the parameters ψ, i^*, and r^* in the equation

$$r_{CB} = \max\{0; r^* + i + \psi(i - i^*)\}, \tag{3.2}$$

based on an inflation rate scenario i given in Figure 3(f). Figure 3(g)-(i) illustrate the same type of reasoning concerning the range of trajectories for real GDP growth rate g based on a plausible investment ratio κ and the variation of parameters δ and ν. Other types of parameterizations are presented in the appendix.

The set of all default parameter values, as well as the lower and upper bounds of their definition intervals used in the sensitivity analysis, are provided in Table 3 (Appendix A). We do not present all the pre-determination of parameter intervals shown in Table 3 here, but Figures SM2 and SM3 in Supplementary Materials illustrate other types of reasoning used, similar to those explained in Figure 3.

3.2. Definition: Sobol indices. The analysis method we employ is a variance-based sensitivity analysis, specifically Sobol' Sensitivity Analysis implemented in the SALib library [42, 46, 43, 44, 28, 32]. This type of method quantifies the variations in the output quantities based on the variations in the input quantities. To do this, we proceed in three steps.

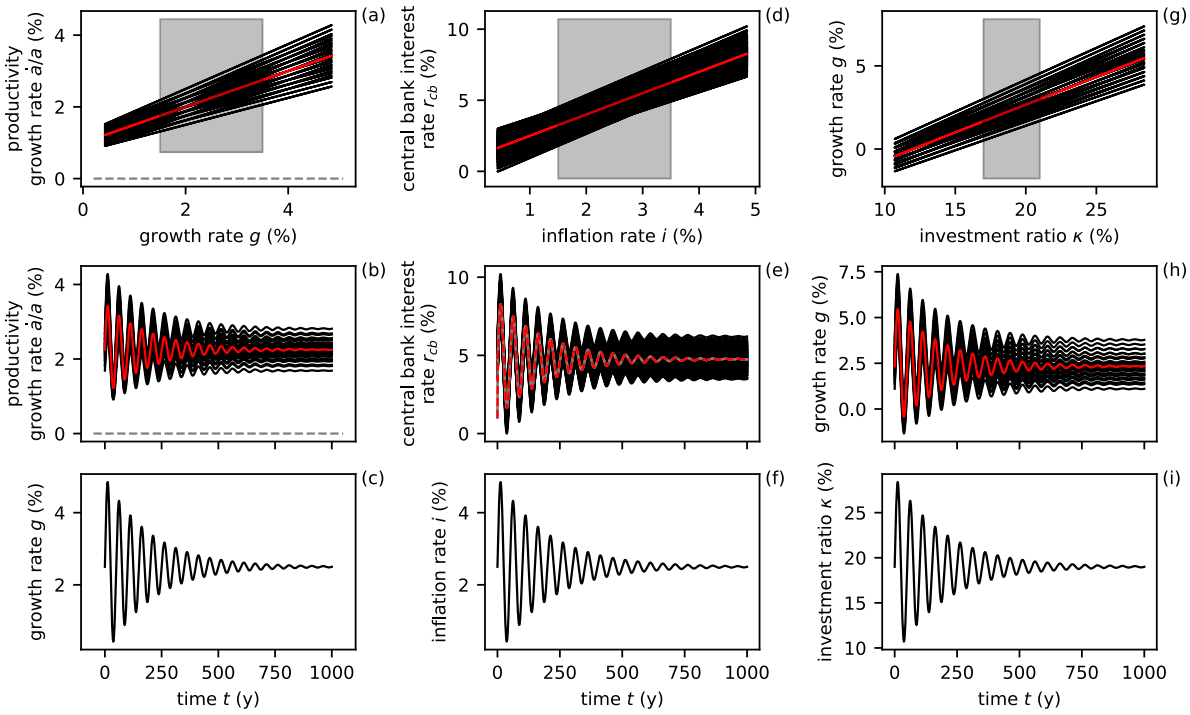

Figure 3. *Pre-determination of the trajectories of output quantities and their value ranges that are explored when varying the associated input parameters. These trajectories are computed from plausible scenarios depicted in (c), (f), and (i). Figures (a)-(b) predict the fluctuation of the labor productivity growth rate $\dot{a}/a$. Figures (d)-(e) predict the fluctuation of the central bank interest rate denoted r_{cb}. Figures (g)-(h) predict the real* GDP *growth rate denoted g. The red curves represent the trajectories computed with the default parameters. The parameters, their default values, and their value intervals are provided in Table 3 (Appendix A).*

First, we begin by determining a sample of values that the input parameters will take, selected from within their respective predetermined expected intervals of variation as described in subsection 3.1. This sample is established using the interval bounds with a Saltelli-type sampling method [46, 43, 44, 9]. Secondly, we conduct simulations starting from identical initial conditions while varying the model parameters' values, and calculate and save the 14 output quantities. Finally, we perform the sensitivity analysis based on these data.

Let f be a function defined on $\mathbb{R}^m$ and $y = f(x) \in \mathbb{R}$ for any $x \in \mathbb{R}^m$. Sobol indices measure the individual contribution of each input variable x (or group of variables) to the output variance of each variable y, accounting for interactions with other variables (or group of variables).

Note that the terms "variables" and "parameters" may be confusing here. Indeed, in the sensitivity analysis presented in this paper, the input variables x of the function f will represent a parameter (or a group of parameters) of the model (2.21)-(2.28), such as capital depreciation δ or the capital-to-output ratio ν. Then, the output y of the function f will correspond to any of the 14 outputs introduced in subsection 3.1, such as the degree of convergence toward the asymptotic limits C or the main frequency of oscillations Ω. Finally, the function f

will represent the map that associates a value of the output y to a given group of model parameters x, by solving the dynamical model (2.21)-(2.28) while keeping other parameters fixed and using a fixed initial condition; see Table 4 (Appendix A). To summarize, the term "input variables" in this section will refer to the IDEE model parameters, while "outputs" will refer to the output quantities defined in subsection 3.1.

Let $u \subset \{1, \dots, m\}$ be a group of indices and u^c, its complement in the set of all indices of the input variables (model parameters) of the function f, i.e., $u^c = \{1, \dots, m\} \setminus u$. The first-order Sobol index $\mathrm{S1}_u$ is defined by the equation

$$\mathrm{S1}_u = \frac{\mathrm{Var}_u(\mathbb{E}_{u^c}[y \mid x_u])}{\mathrm{Var}(y)},$$

where Var is the variance and $\mathbb{E}$ is the expected value. The added indices to the variance and expectation value indicate the model parameters (input variables) with respect to which the variance or expectation value is taken. The index S1 measures the sensitivity of the output variance explained by the variables within the group u.

Second-order Sobol indices S2 quantify the output variance that is explained solely by the interactions between pairs of input variables (or group of variables). For any sets $u, u' \subset \{1, \dots, m\}$, such that $u \cap u' = \emptyset$, it is defined by the equation

$$\mathrm{S2}_{u,u'} = \frac{1}{\mathrm{Var}(y)} \sum_{v \subset u \cup u'} (-1)^{(\#u \cup u' - \#v)} \mathrm{Var}_v(\mathbb{E}_{v^c}[y \mid x_v]).$$

where $\#u$ represents the cardinal of set u. Finally, the total-order Sobol index ST represents the overall contribution of an input variable (or group of variables), including all possible interactions with other variables (or group of variables). In other words, the index ST_u is the part of the output variance that cannot be explained without the group of variables indexed by u. It provides a comprehensive measure of the variable's impact on the output, considering all sources of variation. The total-order Sobol index ST can be formally defined by the equation

$$\mathrm{ST}_u = 1 - \mathrm{S1}_{u^c},$$

thanks to u^c, the complement of set u.

3.3. Robustness. The SALib library [42] provides a way to know each confidence interval during the computation of the Sobol indices (with a typical confidence level of 95%). Given a sequence of M first order Sobol indices S_u^i, $i = 1, \dots, M$ computed for a group of input variables $u \subset \{1, \dots, m\}$, we define the confidence interval I_u with a confidence level of $1 - \alpha$ by the equation

$$I_u = \left[\bar{S} - \epsilon \frac{\sigma}{\sqrt{M}}, \bar{S} + \epsilon \frac{\sigma}{\sqrt{M}} \right],$$

where ϵ is the quantile of order $1 - \alpha/2$ of the unit normal distribution, and where σ (respectively $\bar{S}$) denotes the empirical standard deviation (respectively mean) of the sequence S_u^i, $i = 1, \dots, M$.

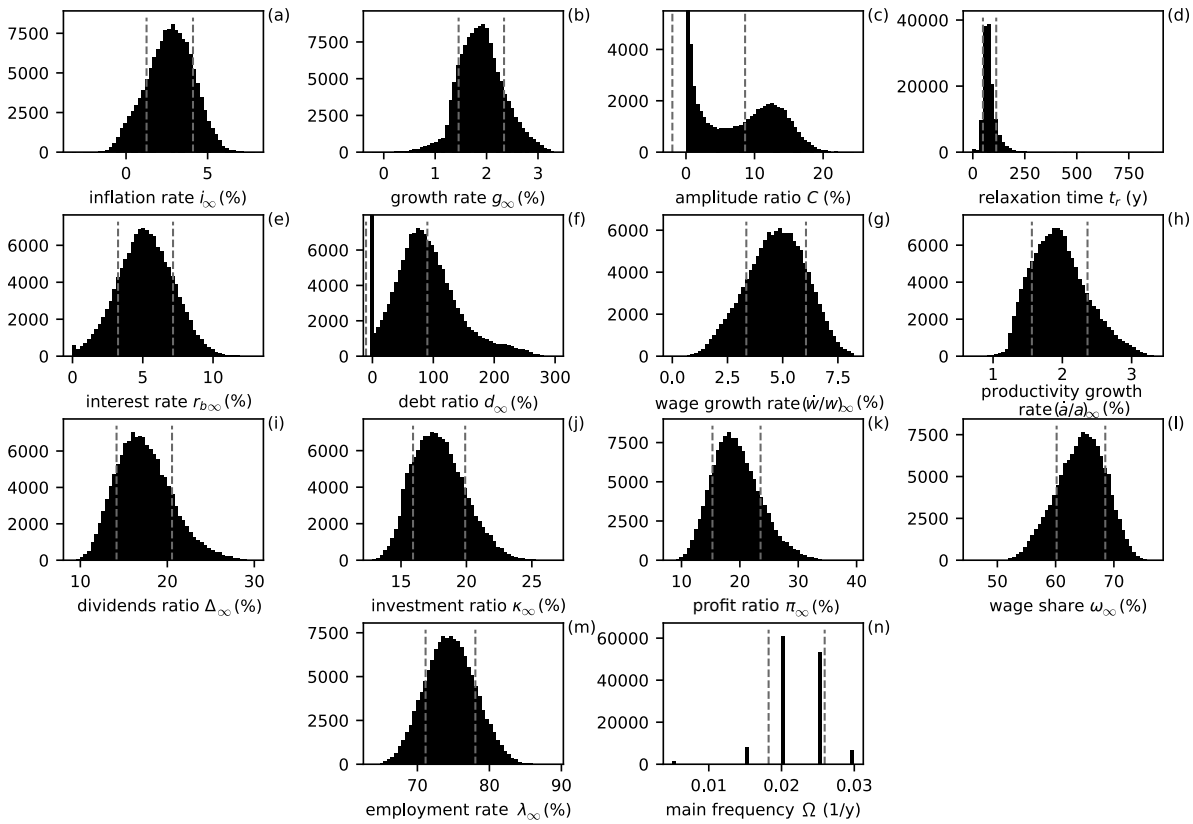

Figure 4. *Histograms of the 14 output quantities computed as part of the sensitivity analysis conducted on a sample of 147456 model parameter sets. All these histograms (except histograms (c), (d), and (n)) correspond to the average values computed over the last simulated century.*

When performing a sensitivity analysis, we obtain the influence of each variable (or group of variables) and we propose a ranking of these groups thanks to the descending order of their respective Sobol indices. We quantify the robustness of the influence ranking of these groups in terms of their impact on the variances of the output quantities. To do this, we define two criteria by using the error bars provided by the sensitivity analysis results; these two criteria are defined and quantified for each output quantity. We first quantify the robustness of the ranking of a pair of parameter groups. This is defined as follows. We have $m = 8$ parameter groups and denote the set of parameter groups by $\mathcal{G}$. For any pair of groups $(u_i, u_j) \in \mathcal{G}^2, 1 \leq i < j \leq m$, we study the gap between the two total-order Sobol indices $|\mathrm{ST}_i - \mathrm{ST}_j|$. We compare this gap to the confidence intervals I_i et I_j computed during the computations of indices with a confidence level of 95%. By summing these two confidence intervals, we get the total confidence interval $I_i + I_j$. The ratio of the gap on the total confidence interval allows us to define the robustness of the ranking of pair (u_i, u_j), denoted

$\rho_{i,j}$:

$$\rho_{i,j} := \frac{|\mathrm{ST}_i - \mathrm{ST}_j|}{I_i + I_j}.$$

Finally we bin this continuous robustness index into three categories: $\rho_{i,j} > 2$ (high robustness), $2 \geq \rho_{i,j} \geq 1$ (medium robustness) and $\rho_{i,j} < 1$ (low robustness). This is visually represented by squares of various colors in the $m \times m$ matrices used below to summarize the pair by pair ranking robustness analysis: light green (high robustness), dark green (medium robustness) and red (low robustness).

Thereafter, for each output quantities like debt ratio d or wage share ω, we define a rough robustness criterion, called general robustness ratio ρ. This criterion allows for a rough quantification of the robustness of the ranking of all the groups of parameters relative to each other. It is defined as the fraction of pairs of groups for which the ranking is robust (greater than 1), i.e.,

$$\rho := \frac{\#\left\{(u_i, u_j)_{1 \leq i < j \leq m} \in \mathcal{G}^2 \mid \rho_{i,j} > 1\right\}}{\#\left\{(u_i, u_j)_{1 \leq i < j \leq m} \in \mathcal{G}^2\right\}},$$

where # stands for the cardinal of the set. For a quick visual grasp of this global ranking, ρ is also binned in five categories: red, orange, yellow, dark green, light green from 60% to 100% by intervals of 10% (rates lower than 50% are included in the first category).

4. Results.

The analysis presented here is based on a computational code of IDEE, which relies on the time discretization of the 10 differential equations introduced in subsections 2.1 and 2.3, under the assumptions outlined in subsection 2.4. These assumptions lead to a reduced form of the model that excludes the climate-related features of the dynamics. These climate aspects have been extensively analyzed in previous studies [4, 6, 5], particularly in the latest version in [37]. The simulations in the current section have been set with parameters and groups of parameters presented in Tables 2 to 4; see Appendix A.

4.1. Sensitivity analysis by group.

We begin by presenting the results of a first sensitivity analysis conducted using a sample of 147 456 simulations. The histograms of the output quantities presented in subsection 3.1 are shown in Figure 4. The sample has been built using Saltelli's sampling scheme [46, 43, 44, 9] that extends Sobol's sequence in a way to reduce the error rates during the computation of Sobol indices. We have chosen the number of simulation (or input sets) to ensure the confidence intervals are small enough to build a ranking of groups by order of influence on output variations. The exact number of simulations is directly determined by the screening method.

In Figure 4, the output quantities are ranked by robustness according to a method that is detailed in subsection 3.3. The histograms represent the range of values taken by the average values computed over the last simulated century of the various presented trajectories, except for Figure 4(c, d, n), which correspond respectively to the amplitude of the oscillations of the trajectories, the relaxation time towards their asymptotic limit, and the main frequency of the oscillations. In each of these histograms, the two vertical dotted lines correspond to the lower and upper quartile values, indicating that 50% of the simulations fall between these two lines.

Figure 4 shows that the simulations are well-controlled in terms of output variation; most of them seem to follow a normal law, at least approximately. This is the result of the precise calibration of the parameter value intervals described earlier. However, some interesting exceptions can be observed.

Firstly, the histogram of the real GDP growth rate g_∞, Figure 4(b), does not exhibit a normal distribution. There is a significant deviation on the left side around g_∞ =1.25%. This break in the slope is related to the one observed in the labor productivity growth rate $(\dot{a}/a)_\infty$, Figure 4(h), which is natural since the latter directly depends on the GDP growth rate.

Secondly, the amplitude ratio C, Figure 4(c), shows that many simulations have strongly converged toward their point of attraction, as many simulations have an amplitude ratio C close to 0%, while fewer simulations are around 20%. Somewhat surprisingly, the amplitude ratio has a local maximum around 12%.

Thirdly, the relaxation time t_r, Figure 4(d), does not follow a normal distribution but rather a kind of decreasing exponential distribution with a wide range of values (from about 50 to over 750 years), yet it is extremely concentrated around 86 years (more than half of the relaxation times fall between 53 and 118 years).

Fourthly, a significant number of simulations resulted in a convergence point with zero debt, as materialized by the vertical bar at 0 in Figure 4(f). This is not particularly surprising but noteworthy.

Finally, the sample of parameter values we established resulted in the exhibition of six main frequencies Ω of the trajectory oscillations (Figure 4(n)), but the majority of the simulations showed two main frequencies at 0.02 and 0.024497 y^{-1}, corresponding to oscillation periods of 50 and 41 years.

4.1.1. Analysis of the three main variables. Figure 5 presents detailed results of the sensitivity analysis of the average value computed over the last century for the three main variables: the private debt ratio d_∞ (Figure 5(a)-(c)), the wage share ω_∞ (Figure 5(d)-(f)), and the employment rate λ_∞ (Figure 5(g)-(i)).

A clear trend emerges when analyzing total-order Sobol index ST: the most influential groups are the first five groups from the left (capital K, inflation i, investment I, productivity p, dividends D), while the influence of the last three groups is more marginal (population N, Phillips curve P, and interest rate r). The dividend group D and the capital group K are the two most impactful groups for all three variables, as evidenced by the significant value of first-order Sobol indices S1 (Figure 5(b, d, f)), with a strong component from the investment group I—it also stands out in the total order—for the debt ratio d_∞ (Figure 5(b)) and productivity p in the wage share ω_∞ (Figure 5(e)). Considering second-order Sobol indices S2, the combination of the two groups (K, D) emerges as the most impactful (Figure 5(c, f, i)).

The order in which the variations of the input parameter groups impact the variations of the output quantities is determined by the significance of the total-order Sobol index (Figure 5(a, d, g)). For the debt ratio d_∞, the wage share ω_∞, and the employment rate λ_∞, the rankings from the most to the least impactful groups are respectively D, K, I, p, i, r, P, N for d_∞ and D, K, p, i, I, r, P, N for both ω_∞ and λ_∞.

Figure 6 is a graphical representation of the robustness (see subsection 3.3) of the ranking

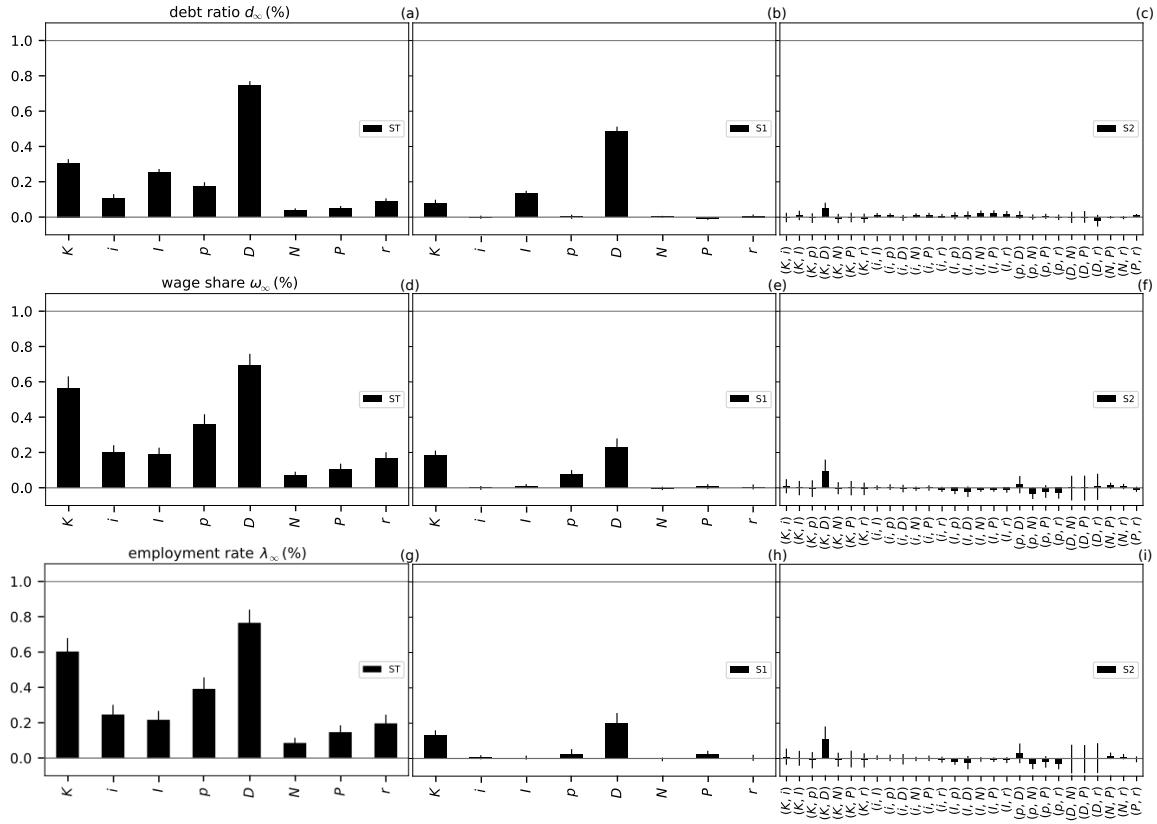

Figure 5. *Results of the sensitivity analysis for the average value computed over the last century for the three main variables of the model: the private debt ratio d_∞ (figures. (a)-(c)), the wage share ω_∞ (figures. (d)-(f)), and the employment rate λ_∞ (figures.(g)-(i)). Figures (a, d, g) represent the total-order Sobol indices ST; Figures (b, e, h) show the first-order Sobol indices S1; while figures. (c, f, i) depict the second-order Sobol indices. For each index, an error bar (a black vertical line at the top of the thick bars) is associated.*

of parameter groups by their influence in the variation of the three output quantities. The general robustness ratios ρ for the three output quantities are quite high: very high for the debt ratio d_∞ (92.9%), and relatively high for the wage share ω_∞ and the employment rate λ_∞ (78.6%). We observe that the two pairs of parameter groups (r, i) and (P, N) are consistently difficult to rank because their total-order Sobol indices ST are within less than one confidence interval of each other (Figure 6(a)-(c)). These triangular robustness matrices differ significantly between the debt ratio d_∞ on one hand (Figure 6(a)), and the wage share ω_∞ and employment rate λ_∞ on the other (Figure 6(b)-(c)). In fact, we will see in the analysis of the results considering all parameter groups that the sensitivity analysis profiles belong to two different categories.

4.1.2. Group analysis and classification of total-order Sobol indices into five categories.

Total-order Sobol indices. Figure 7 presents profiles of total-order Sobol indices classified into five categories and illustrated by different colors. These categories have been identified by

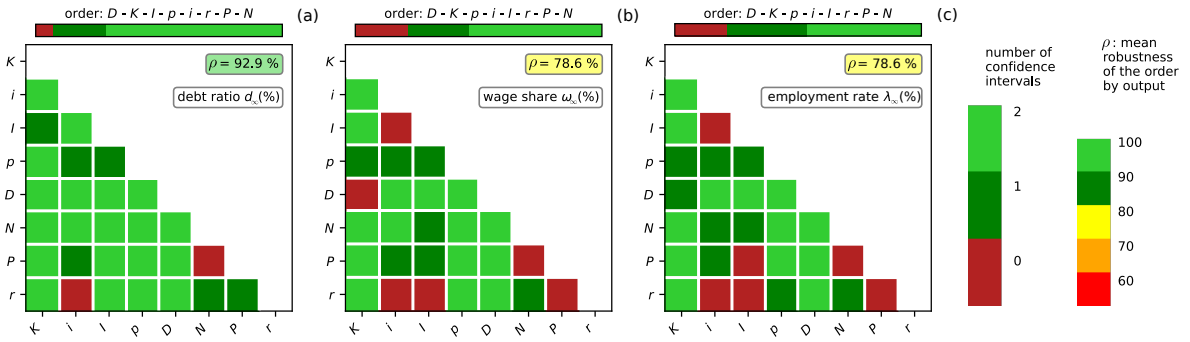

Figure 6. *Robustness of the influence ranking of parameter groups for asymptotic values of (a) the debt ratio d_∞, (b) the wage share ω_∞ and (c), the employment rate λ_∞. Each colored square indicates the gap between two levels reached by the total-order Sobol indices of parameter groups (the thick bars in Figure 5). If a square is light green, the gap between the two indices is greater than or equal to two total confidence intervals; if a square is dark green, the observed gap lies between one and two; and if the square is red, then the gap is less than one. The percentage ρ quantifies the general robustness ratio of the classification of parameter groups by output quantity. It is calculated as the ratio of the number of pairs of parameter groups whose index difference is greater than at least one confidence interval to the total number of pairs. The horizontal colored bars above the triangular matrices provide a visual representation of the distribution of pairs below, at one, or above two total confidence intervals.*

direct inspection, an exercise much simpler at the group level than at the individual parameter level. This classification into five categories is shown here by group but also by parameter in the next section once the main groups are isolated; see subsection 4.1.3.

Among these categories, the first and largest includes five output quantities (Figure 7(a)-(e)): dividend ratio Δ_∞, investment ratio κ_∞, wage share ω_∞ and employment rate λ_∞, and profit ratio π_∞. Thus, this category includes two of the three main variables of the model (λ_∞ and ω_∞). This category is characterized by the dominance of two groups: the dividend parameters group D and the investment parameters group K, with a third group, the labor productivity p playing a lesser but still significant role. Additionally, this category is distinguished by the influence of the inflation parameters group i and the investment group I, and the three least influential groups: population N, profit P, and interest rate r.

The second category includes three output quantities: the inflation rate i_∞, the wage growth rate $(\dot{w}/w)_\infty$, and the interest rate r_∞ (Figure 7(e)-(g)). This group is characterized by also having D and K as the main groups, but in reverse order compared to the first category (this time, the dominant group is K). Additionally, the difference from the first category is that the other groups are much less impactful, except for the investment group I on the variation of the interest rate r_∞ (Figure 7(g)).

The third category (Figure 7(h)-(j)) consists of the amplitude ratio C, relaxation time t_r, and main frequency Ω. In this category, the three main groups are investment I, productivity p, and dividends D, with the capital group K now ranked lower compared to its position in the first two categories. The groups N, P, and r remain less impactful on the variations in output quantities.

The fourth category includes the growth rate g_∞ and labor productivity growth rate

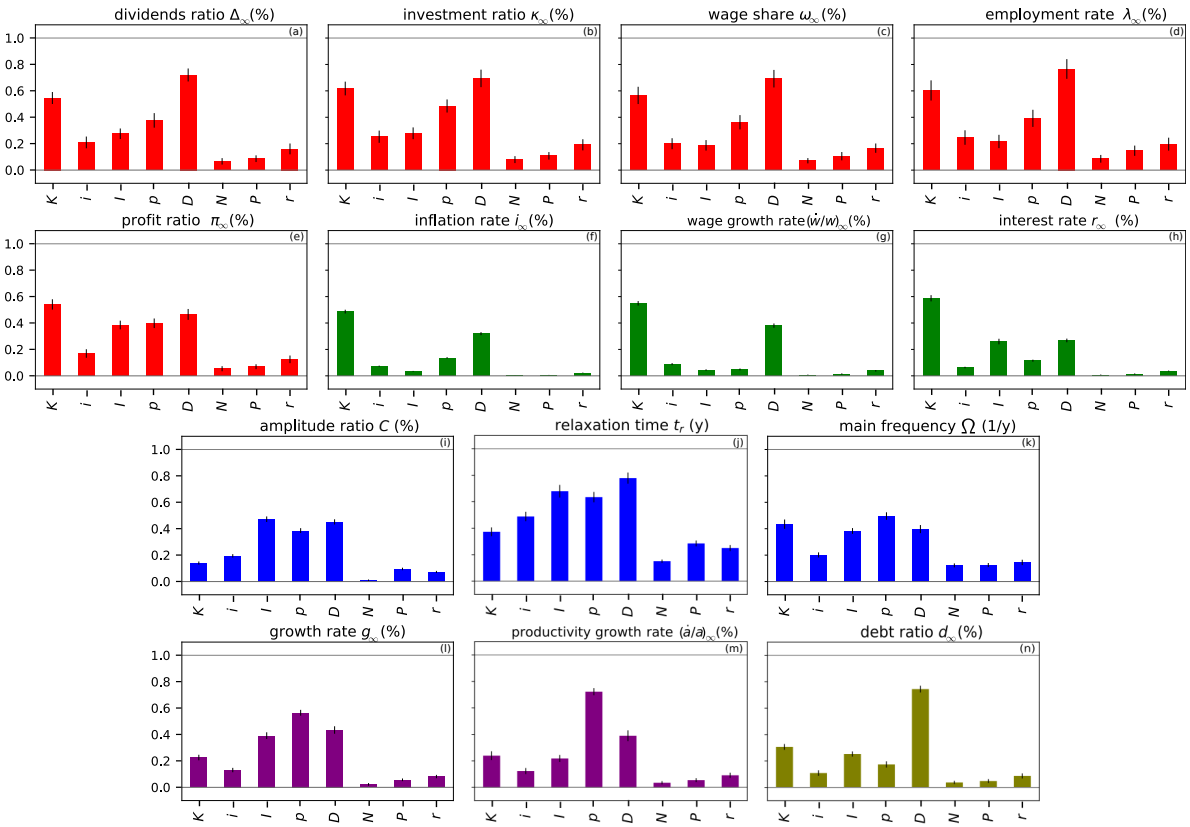

Figure 7. *Total-order Sobol indices of parameter groups by output quantity. The outputs are classified into five categories: : the first category (a)-(e), the second category (f)-(h), the third (i)-(k), the fourth (l)-(m), and the last category consisting only of the debt ratio d_∞ (n).*

$(\dot{a}/a)_\infty$ (Figure 7(l)-(m)). This category resembles the third category but differs in that the group K becomes relatively impactful again, in proportions similar to those of the three groups I, p, and D.

The fifth category includes only one of the three main variables: the debt ratio d_∞ (Figure 7(n)). It is characterized by having one very dominant group among all others: the dividend parameters group D for the debt ratio and the productivity parameters group p for the productivity growth.

The distinction into five categories highlights which sets of output variables react similarly to changes in the model parameters. This in itself may lead to reinvestigate some of the model choices if some of these correlated outputs changes appear suspicious on general macroeconomics ground to the modeler. We did not pursue this direction of investigation very far for the present model, but we make further comments on how this may be achieved in practice in subsection 5.1.

Robustness. The robustness matrices for the ranking of groups by their influence on output quantities are shown in Figure 8 for the five categories.

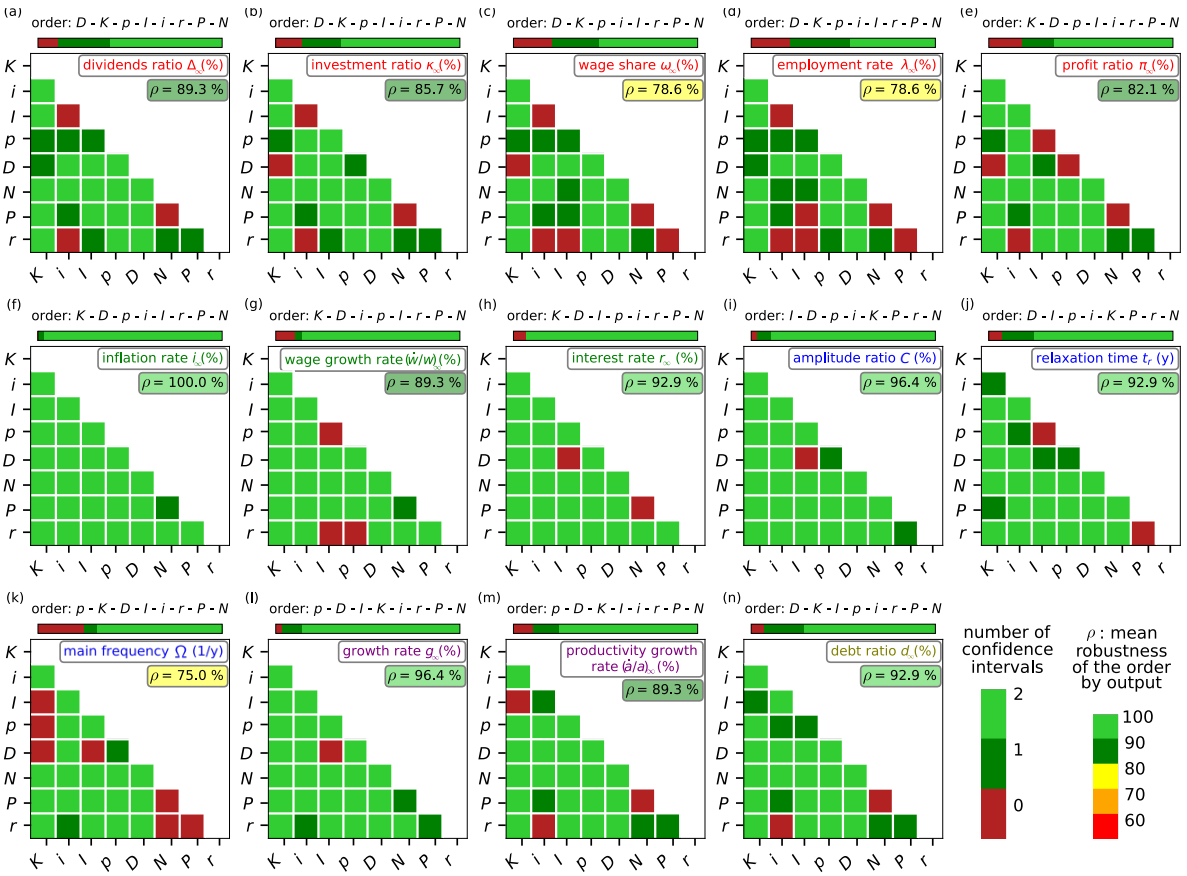

Figure 8. *Robustness of the influence ranking of parameter groups for all output quantities. The different graphs are classified according to the five presented categories: the first category (a)-(e), the second category (f)-(h), the third (i)-(k), the fourth (l)-(m), and the last category consisting only of the debt ratio d_∞ (n).*

Overall, a high level of general robustness is observed, with average robustness levels between $\rho = 75\%$ and 100% (Figure 8(k, f)). The robustness matrices are relatively similar between output quantities within categories. The set of robustness matrices clearly shows that the workforce group N, the profit group P, and the interest group r are the three least impactful groups (Figure 7) and the hardest to classify among each other; see, for example, the red squares in the lowest row (Figure 8(c, d)).

The first category (Figure 8(a)-(e)) has the lowest robustness ratio at 82.9%, but this is primarily due to the three least impactful groups. Apart from these three groups, the link between investment I and inflation groups i must be clarified, except for the profit ratio output; see Figure 8(a)-(d). Similarly, the order between groups D and K should be studied (Figure 8(b, e)).

The second category (Figure 8(f)-(h)) presents the highest level with an average robustness of 94.1%. Excluding again the three least impactful groups, there remains ambiguity between

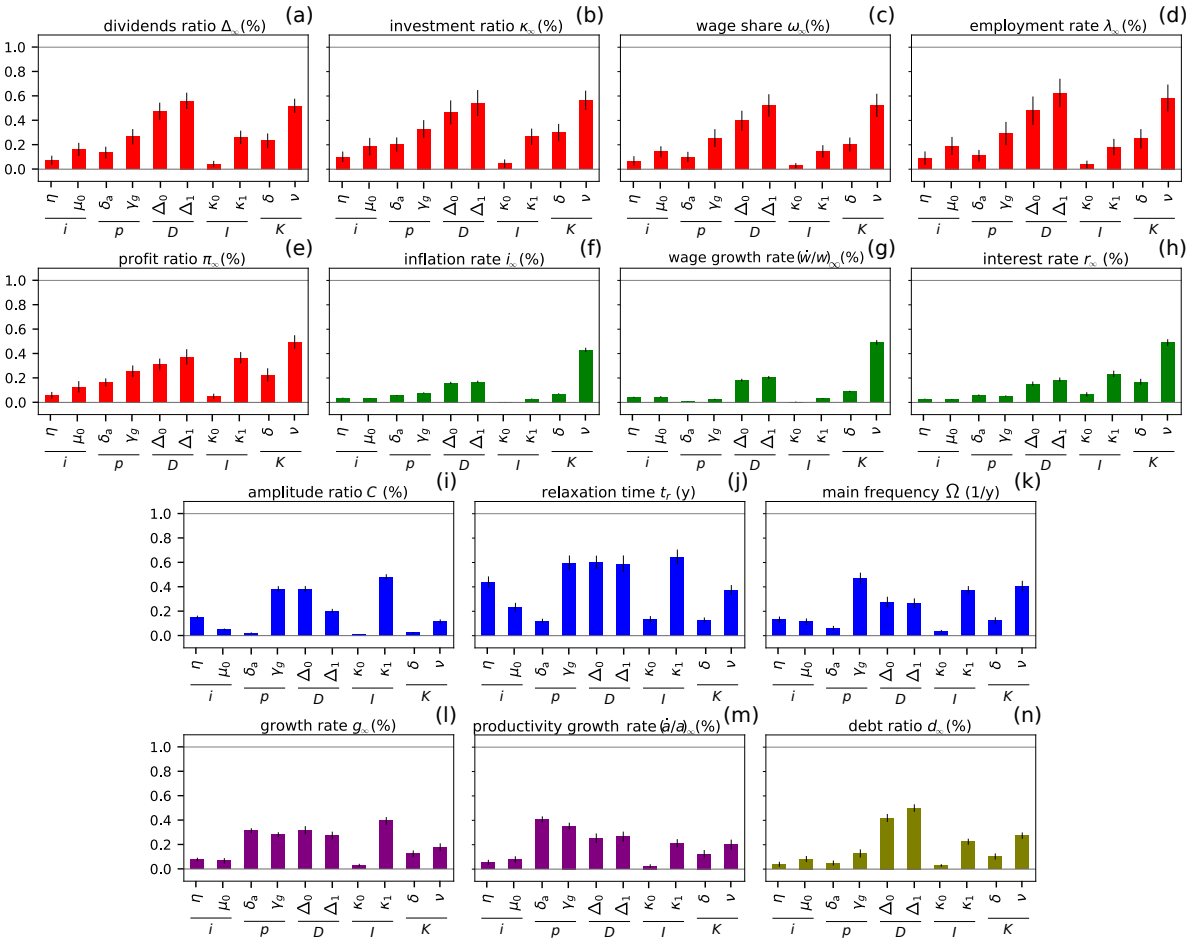

Figure 9. *Total-order Sobol indices of parameters for the five main groups: inflation rate i, productivity p, dividends D, investment I, and capital K and all output quantities. The outputs are classified into five categories: : the first category (a)-(e), the second category (f)-(h), the third (i)-(k), the fourth (l)-(m), and the last category consisting only of the debt ratio d_∞ (n).*

the productivity group p and the investment group I (Figure 8(g)) and between the dividend group D and the investment group I (Figure 8(h)).

The third category (Figure 8(i)-(k)) shows a relatively high level of robustness with two matrices that are very similar Figure 8(i, j) and a third that differs from the others (for the main frequency Ω Figure 8(k)). In this last case, there is significant difficulty in the ranking of the groups K with I, p, and D that we need to address.

The fourth category (Figure 8(l)-(m)) shows a very high level of robustness ($\rho = 92.85\%$) with only one ambiguity between the groups D and I (Figure 8(l)) and between K and I (Figure 8(m)). Finally, the last category, consisting only of the private debt ratio d_∞ (Figure 8(n)), is very robust when the three groups N, P, and r are excluded from the analysis.

4.1.3. Parametric analysis.

Total-order Sobol indices. The most significant result from the previous study is that out of the eight parameter groups, only five significantly impact the variations in the outputs. Therefore, we can eliminate the three groups N, P, and r, and focus our study on the other groups. This involves conducting an analysis that includes each parameter from these groups, reducing the analysis to the eight parameters that comprise the groups i, p, D, I, and K. We ran 90 112 simulations, varying the eight parameters within the bounds specified in Table 3 (Appendix A). The exact number of simulations is directly determined by the screening method; see e.g., [46, 43, 44, 9].

Figure 9 shows profiles of total-order Sobol indices and is similar to Figure 7 but displays the results by parameter and by parameter group. Again, we classify the 14 output quantities into five categories, which coincide with the categories we identified earlier.

Regarding the first category (Figure 9(a)-(e)), we observed in Figure 7 that the dominant groups were the dividends parameters group D and the capital parameters group K. The parameter-by-parameter analysis given in Figure 9 confirms this trend and refines it by showing that the impact of group D is particularly driven by the slope of the linear curve Δ_1, with a significant influence from the intercept Δ_0 as well. Similarly, the impact of group K is mainly driven by the parameter ν (output-to-capital ratio). Regarding the ambiguity between the groups I and i, we observe that the parameter dominating the other three is κ_1, which dictates the slope of the linear investment function. Following that is the constant in the price markup μ_0, which belongs to the inflation group.

The other parameters have a more or less significant impact and are relatively homogeneous within the same group. Notably, there is a significant difference within the investment group I, where the two parameters have very different levels of influence; the slope κ_1 is much more impactful than the intercept κ_0 (see, for example, Figure 9(e)).

In the second category (Figure 9(f)-(h)), the same groups K and D remain dominant, with a strong representation of the parameter ν. However, the other groups have a minimal impact, much more than in the first category. Regarding the ambiguities observed in Figure 8 for this category, we begin by noting that the groups p and I are difficult to classify for the wage growth rate $(\dot{w}/w)_\infty$ (Figure 9(g)) because both are very negligible. This is not the case for groups D and I for the interest rate r_∞, which shows that the parameter κ_1 is again important, even though the two parameters of group D follow closely behind (Figure 9(h)).

The third category of output quantities (Figure 9(i)-(k)) shows a quite different profile in the total-order Sobol indices compared to the other two categories. The most significant groups are p, D, and I but they remain difficult to sort within this category. The investment group I is particularly impactful, again especially due to the slope κ_1. The labor productivity parameter group p is also significant, primarily through the parameter γ_g, which introduces the dependence of productivity growth on the growth rate g_∞. The ambiguity that exists among these three groups and the group K seems to be resolved for the amplitude ratio C and the relaxation time t_r (Figure 9(i, j)) because each of the three groups has a parameter that has a total-order Sobol indexe above those to the two parameters of group K. However, this is not the case of the group K for main frequency Ω (Figure 9(k)), which is only surpassed by the parameter γ_g.

The profiles of the fourth category (Figure 9(l)-(m)) are similar to those of the third but

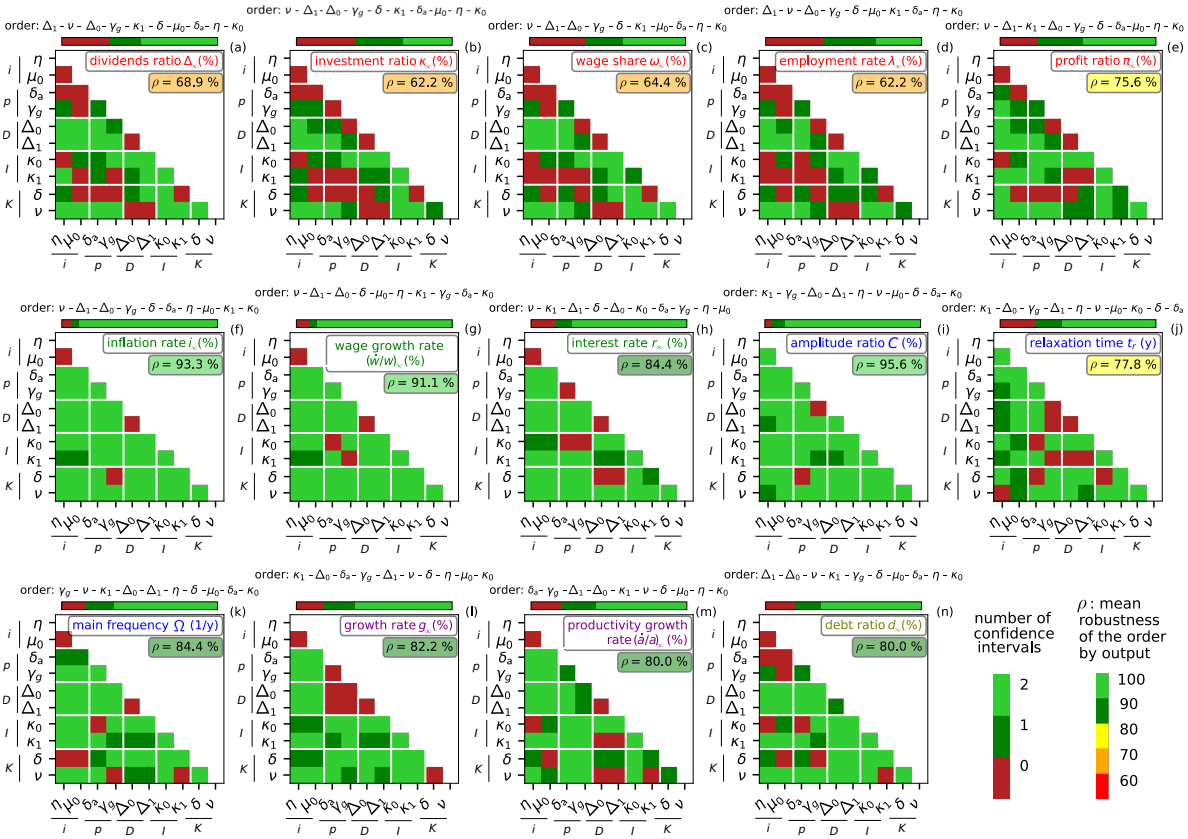

Figure 10. *Robustness of the influence ranking of parameters for the five main groups and all output quantities. The different graphs are classified according to the five presented categories: the first group (a)-(e), the second group (f)-(h), the third group (i)-(k), the fourth group (l)-(m), and the last group consisting only of the debt ratio d_∞ (n).*

with the group p being even more dominant, particularly due to the significant impact of the parameter δ_a, which represents the constant growth rate of labor productivity. Regarding the ambiguities between the groups D, I and K, we again notice that the group I is clearly dominant via the parameter κ_1 for the growth rate g_∞ (Figure 9(l)), while the group K only dominates the inflation group i.

Finally, the last category, which consists solely of the debt ratio d_∞ (Figure 9(n)), is predominantly dominated by the dividend parameter group D. However, it also reveals that for the I and K groups, the parameters κ_1 and ν are crucial.

Robustness. Let us now analyze the robustness of the ranking by influence that can be made of the parameters for each output quantity (this ranking is displayed for each output quantity in Figure 10). A general observation from Figure 10 indicates that the ranking is somewhat less robust than that by groups illustrated in Figure 8, but it remains satisfactory, with a general robustness exceeding 60% for the wage share ω_∞ and the employment rate λ_∞, and over 80% for the debt ratio d_∞; see also Figure 10(c, d, n).

The first category (Figure 10(a)-(e)) is the one where the ranking is the least robust, standing just above 60%. However, it is evident that the parameters from the dividends group D and the output-to-capital ratio ν consistently rank among the top three parameters with strong robustness, except for the profit ratio, where the parameter Δ_0 is slightly overtaken by the investment slope κ_1; see Figure 10(e).

The second category (Figure 10(f)-(h)), in contrast, presents the most robust parameter rankings, exceeding 84% general robustness, with a general robustness percentage even reaching 93% for the inflation rate i_∞ (Figure 10(f)). We observe a similar leading trio as in the first category. The third category (Figure 10(i)-(k)) follows closely behind the second in terms of robustness, also exceeding 84%, and even achieving the maximum value for the amplitude ratio C (Figure 10(i)). Additionally, we find high general robustness ratios concerning the fourth (Figure 10(l)-(m)) and fifth categories, both above 80% (Figure 10(n)).

5. Discussion.

5.1. General comments. Each of the robustness matrices presented in Figure 10 enables the modeler to evaluate the significance of modifications to one or more parameters on the output quantities for which such an analysis has been conducted. For example, in the case of the IDEE computational code, altering the parameter for the slope of the investment curve κ_1 will have a substantial influence on the amplitude ratio C (Figure 10(i)), the relaxation time t_r (Figure 10(j)), and the growth rate g_∞ (Figure 10(l)), as this parameter ranks first in the classification of these three outputs. However, it will have virtually no impact on the inflation rate i_∞, where κ_1 ranks second to last (Figure 10(f)).

More generally, the two-level analysis (parameter groups and individual parameters) has at least two purposes:

- It allows the modeler to make a first selection of important parameters at the group level in a faster way, especially when the number of parameters is large (which is only marginally the case for the IDEE model)
- the identification of important parameters and parameter groups points towards parts of the model that need special attention, and possibly more precise modeling. For example, if some important parameters (i.e., whose value are particularly critical on the model output) relate to equations that are too crudely modeled, improving on the model would most likely be the most efficient action to improve the model reliability, and not simply try to calibrate these parameters in a more precise manner.
- The identification of similar output behaviors, that lead here to the definition of five output categories, is more easily performed at the group level than at the individual level. This identification may also help to improve the model itself, in a more precise way than the previous step, by addressing questions such as: is the difference of behavior between groups an intrinsic macroeconomic feature or a model-dependent one?

5.2. Class-struggle dynamics. Note that we find that the most influential group of parameters in the model is related to shareholder dividends D (see for example Figure 5), which represents in the model the portion of surplus value that is distributed to owners rather than workers. This clearly reflects the class-struggle dynamic characteristic of models based on the

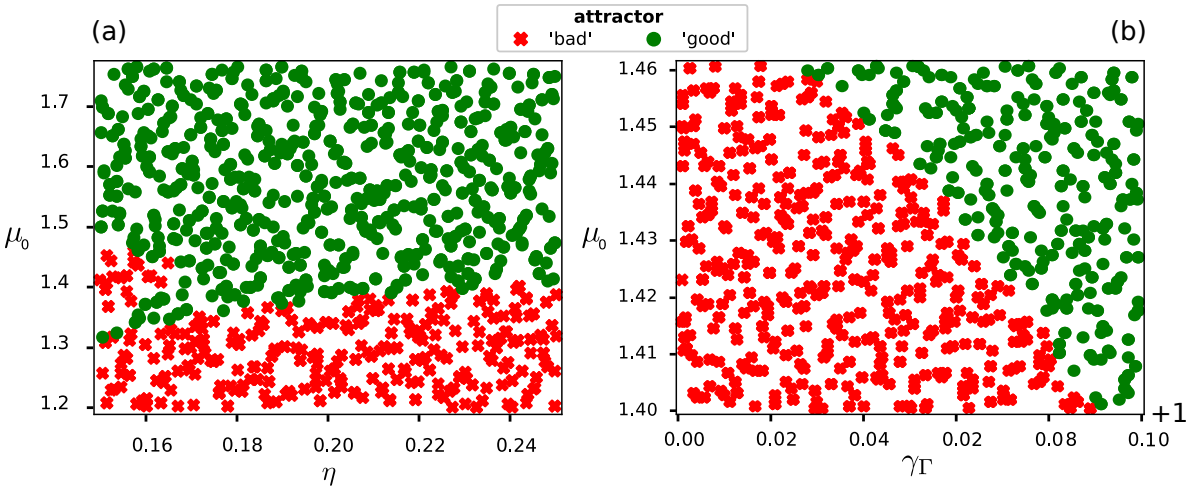

Figure 11. *(a) Graphical representation of whether the simulations converge towards the "good" (green) or "bad" (red) attractor depending on the values of the pairs (η, μ_0). In these 1 000 simulations, the other parameters are set to their default values. (b) Graphical representation of whether the simulations converge towards the "good" (green) or "bad" (red) attractor depending on the values of the pairs (γ_Γ, μ_0). The other parameters are set to their default values; see Table 3 in Appendix A.*

Goodwin-Keen framework [19, 1, 53, 34].

5.3. Criticality of the price markup. We revisit here the criticality of the price markup μ_0, as highlighted in Bolker et al. (2021) [2], regarding the attraction basin of the "good" attractor (i.e., where the equilibrium point is of the Solow type). This study confirms that μ_0 is the most influential parameter in determining whether the simulation converges to the "good" or "bad" equilibrium. We also find this result, as illustrated in Figure 11(a), which clearly shows a sharp separation between simulations converging toward the "good" and "bad" equilibria within the range $1.3 \leq \mu_0 \leq 1.4$, for the other parameters set to their default value except η. A slight influence of the parameter η around the value 0.16 is observed, but it remains minor compared to the overwhelming influence of μ_0.

Our sensitivity analysis provides additional insight into the importance of the parameter μ_0. Indeed, while this parameter is the most influential in determining the attraction basin of the "good" equilibrium, it becomes less important once its value exceeds its critical threshold, i.e., $\mu_0 > 1.6$. This is clearly shown in Figure 10. For example, if we focus on the model's three main variables—debt ratio d_∞ (Figure 10(n)), wage rate ω_∞ (Figure 10(c)), and employment ratio λ_∞ (Figure 10(d))—we observe that the parameter μ_0 ranks only seventh, seventh, and sixth in terms of influence, respectively, and is robustly dominated by the most influential parameters, Δ_0, Δ_1, ν, and even κ_1 for the debt ratio d_∞. Therefore, this observation helps to temper the critical nature of the parameter μ_0. While it is particularly critical, this is true within the attraction basin of IDEE but not for the outputs that are observed here.

The sensitivity analysis we present does not include γ_Γ, the twentieth economic parameter in the IDEE model, which appears in the debt equation as a "forgiveness" coefficient (see

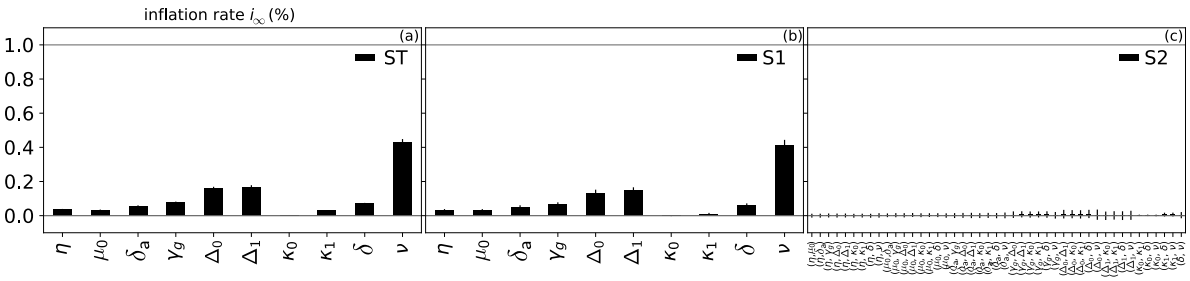

Figure 12. *Results of the sensitivity analysis for the average value computed over the last century for the inflation rate i_∞. Figure (a) represents the total-order Sobol index ST; Figure (b) shows the first-order Sobol indices S1; while Figure (c) depicts the second-order Sobol indices S2. For each indices, an error bar (a black vertical line at the top of the thick bars) is associated.*

(2.10)), reflecting a proportion of debt that is canceled by the creditor. We excluded it from our analysis because this parameter only comes into play when the simulated trajectory approaches the boundary between the "good" and "bad" attractors. As mentioned earlier, the focus of this paper is on the "good" equilibrium. However, it is worth noting that the parameter γ_Γ, like the price markup μ_0, influences slightly the attraction basins despite it is also dominated by μ_0. Figure 11(b) shows that the "forgiveness" parameter counteracts the effect of μ_0 on the basin. The higher the value of γ_Γ, the more it offsets the effect of μ_0.

5.4. First and second order analysis. In the presentation of our results (section 4), we exclusively use the total-order Sobol index ST as the informative measure and thus do not delve into the first-order Sobol index S1 or second-order Sobol index S2. However, these indices can be easily extracted from the data calculated using the SALib library [42]. For instance, we could estimate whether the variance of an output quantity is primarily due to the variance of a single input parameter—this would be indicated by both a high total-order Sobol index ST and a high first-order Sobol index S1. Alternatively, if the variance stems predominantly from interactions between the parameter and other parameters, we would observe a high ST but a low S1. If the interactions are significant at the second-order level, this would be reflected in a high second-order Sobol index S2.

For instance, in the case of the three main variables—debt ratio d_∞, wage share ω_∞, and employment ratio λ_∞—Figure 5(b), (e), and (h) clearly show that the total-order Sobol indices ST are partially explained by the first-order indices S1, particularly for the three main groups: dividends D, capital K, and productivity p. The second-order Sobol indices S2 primarily reveals interactions between the D and K groups (negative values can be considered negligible). However, we can observe that the total index is still significantly higher than the first- and second-order indices, indicating that these variables are strongly influenced by group interactions rather than by independent parameter fluctuations. This is expected for these three output quantities, as their dynamics involve a large number of different mechanisms.

Such a configuration is not, however, encountered systematically. For instance, the sensitivity analysis by parameter—presented in subsection 4.1.3 (as opposed to the one by parameter groups in subsection 4.1.2)—for the inflation rate i_∞ (Figure 12) shows that the

Table 1

Computational aspects of the numerical study presented in the present article. The time step value is $\Delta t = 1/12\,y$ and the number of CPU used is 6. The simulations and sensitivity analysis were performed on one Intel® Core™ i7-1065G7 CPU @ 1.30 GHz × 8.

Nb. of runs	Time for running them all	Time spent per run	Time for post-processing	Time for the SA
90 112	2 h 41 mn 25 s	0.648 s	3 h 11 mn 2 s	19 s
147 456	4 h 25 mn 50 s	0.649 s	5 h 14 mn 32 s	20 s

parameters' influence on the output quantity is almost entirely explained by independent parameter variations, resulting in first-order indices S1 that are very close to the total-order indices. Conversely, the second-order and higher indices are nearly zero. We provide the results of our sensitivity analyses by groups and by parameters for the Sobol indices S1, S2, and ST in the supplementary materials.

6. Computational aspects. This sensitivity analysis of the IDEE computational code was conducted using a code that we are sharing as open-source on GitHub [29]. The sensitivity analysis itself is handled by the SALib library [42, 27, 32] within our code. We developed this code in Python and parallelized it across 6 CPUs. The simulations, post-process, and sensitivity analysis were performed on an Intel® Core™ i7-1065G7 CPU @ 1.30 GHz × 8, with 6 CPUs (out of 8) solely dedicated to computational tasks.

Such a study requires a significant number of simulations: 147 456 for the sensitivity analysis by parameter groups (subsection 4.1.2) and 90 112 for the analysis by individual parameters (subsection 4.1.3). This volume of simulations is feasible with an efficient model code. This is the case for the IDEE computational code that we use, implemented in Fortran 90 and based on a numerical scheme using a Runge-Kutta RK4 method. It computes the solution of the differential equations introduced in subsections 2.1 and 2.3 at each time step. This method ensures numerical accuracy and stability, especially when dealing with the non-linear dynamics inherent in the model. It completes a 1000-year simulation with a 'monthly' time step of $\Delta t = 1/12$ y in an average of 0.648 s. The time step is short enough to adequately capture the most abrupt non-linear economic effects.

Our study relies on the calculation of 14 output quantities, which also involves a substantial amount of post-processing time (3 h 11 mn for 90 112 simulations). The sensitivity analysis itself is very quick, taking only 19 s once the post-processing data is computed. All relevant information regarding computation times is provided in Table 1.

7. Conclusion. This paper presents a sensitivity analysis conducted on 19 parameters of the IDEE model, based on the variations of 14 output quantities, involving approximately 250 000 simulations. After presenting the model's equations, we outlined how to define relevant output quantities for the model's simulated trajectories and explained the process of variance-based sensitivity analysis. Our study complements previous work [4, 2, 37] by focusing primarily on the purely economic aspect of the model.

Our sensitivity analysis led us to identify five influential parameter groups and three less significant ones (Figure 5). We showed how these five groups can then be ranked by influence, and proposed two indices to assess the robustness of this ranking. The main index exceeds

78.6% for the asymptotic values of the model's three main variables (private debt, wage share, and employment rate) (Figures 7 and 10). The outputs can also be grouped into 5 categories that behave in a similar way with respect to changes in the five parameter groups. This highlights how output quantities react collectively and not only individually to parameter changes. Armed with these findings, we next moved to analyze the model sensitivity to individual parameter changes and confirmed the importance of the groups and categories identified in the previous step. We also revisited the critical parameter identified by Bolker et al. (2021) [2] (the price markup) and showed that once its value is set far from the critical zone separating the "good" and "bad" attractors' of the dynamics, it becomes a relatively negligible parameter in determining the asymptotic convergence point. Our study further demonstrates that once this critical the price markup is avoided, the IDEE computational code that we used yields robust results with respect to expected variations in the parameters' values.

We stress again that performing a sensitivity analysis at both the group and individual levels and not only at the individual level as is usually done facilitates the identification of important parameters and of collective output variations with respect to parameter changes, especially for very large models. The first point is the main objective of a sensitivity analysis, while the second one gives a better understanding of the dependence of the dynamics on model parameters, and may possibly help to identify weak modeling choices (see subsection 5.1). This led us to conclude that the IDEE model is robust with respect to the expected domain of variations or uncertainties of its parameters.

We hope this paper will inspire economic modelers to apply such sensitivity analysis methods. To this end, we have made the computational code of the sensitivity analysis we developed available as open-source on GitHub [29].

Acknowledgments. We would like to acknowledge Gaël Giraud for his advice and the discussions we had concerning the mathematical modeling of the IDEE model. We thank the SALib library [42] for providing a powerful open-source tool for sensitivity analysis, which has enabled us to carry out this work.

ORCIDs. Pierre-Yves Longaretti https://orcid.org/0000-0002-9400-287X; Hugo A. Martin https://orcid.org/0000-0002-7089-8958.

REFERENCES

[1] G. A. Akerlof and J. E. Stiglitz, *Capital, Wages and Structural Unemployment*, The Economic Journal, 79 (1969), p. 269, https://doi.org/10.2307/2230168.

[2] B. M. Bolker, M. R. Grasselli, and E. Holmes, *Short communication: Sensitivity analysis of an integrated climate-economic model*, SIAM Journal on Financial Mathematics, 12 (2021), pp. SC44–SC57, https://doi.org/10.1137/21M1404120.

[3] E. Borgonovo, *A new uncertainty importance measure*, Reliability Engineering & System Safety, 92 (2007), pp. 771–784, https://doi.org/10.1016/j.ress.2006.04.015.

[4] E. Bovari, G. Giraud, and F. Mc Isaac, *Coping With Collapse: A Stock-Flow Consistent Monetary Macrodynamics of Global Warming*, Ecological Economics, 147 (2018), pp. 383–398, https://doi.org/10.1016/j.ecolecon.2018.01.034, https://doi.org/10.1016/j.ecolecon.2018.01.034.

[5] E. Bovari, G. Giraud, and F. McIsaac, *Financial impacts of climate change mitigation policies and their macroeconomic implications: a stock-flow consistent approach*, Climate Policy, 20 (2020), pp. 179–198, https://doi.org/10.1080/14693062.2019.1698406, https://doi.org/10.1080/

14693062.2019.1698406.

[6] E. Bovari, O. Lecuyer, and F. Mc Isaac, *Debt and damages: What are the chances of staying under the 2° C warming threshold?*, International Economics, 155 (2018), pp. 92–108, https://doi.org/10.1016/j.inteco.2018.02.002, https://linkinghub.elsevier.com/retrieve/pii/S2110701717302615.

[7] E. Bovari, O. Lecuyer, and F. Mc Isaac, *Debt and damages: What are the chances of staying under the 2°c warming threshold?*, International Economics, 155 (2018), pp. 92–108, https://doi.org/https://doi.org/10.1016/j.inteco.2018.02.002, https://www.sciencedirect.com/science/article/pii/S2110701717302615. Special issue on 'Social values of carbon and climate policy signals in the post-COP21 context'.

[8] R. Calel, S. C. Chapman, D. A. Stainforth, and N. W. Watkins, *Temperature variability implies greater economic damages from climate change*, Nature Communications, 11 (2020), pp. 1–5, https://doi.org/10.1038/s41467-020-18797-8, http://dx.doi.org/10.1038/s41467-020-18797-8.

[9] F. Campolongo, A. Saltelli, and J. Cariboni, *From screening to quantitative sensitivity analysis. A unified approach*, Computer Physics Communications, 182 (2011), pp. 978–988, https://doi.org/10.1016/j.cpc.2010.12.039.

[10] R. I. Cukier, C. M. Fortuin, K. E. Shuler, A. G. Petschek, and J. H. Schaibly, *Study of the sensitivity of coupled reaction systems to uncertainties in rate coefficients. I Theory*, The Journal of Chemical Physics, 59 (1973), pp. 3873–3878, https://doi.org/10.1063/1.1680571.

[11] Y. Dafermos, M. Nikolaidi, and G. Galanis, *A stock-flow-fund ecological macroeconomic model*, Ecological Economics, 131 (2017), pp. 191–207, https://doi.org/10.1016/j.ecolecon.2016.08.013.

[12] Y. Dafermos, M. Nikolaidi, and G. Galanis, *Climate Change, Financial Stability and Monetary Policy*, Ecological Economics, 152 (2018), pp. 219–234, https://doi.org/10.1016/j.ecolecon.2018.05.011.

[13] Department of Economic and Social Affairs, Population Division, *World population prospects 2019 highlights*, tech. report, United Nations, 2019.

[14] S. Dietz and N. Stern, *Endogenous Growth, Convexity of Damage and Climate Risk: How Nordhaus' Framework Supports Deep Cuts in Carbon Emissions*, The Economic Journal, 125 (2015), pp. 574–620, https://doi.org/10.1111/ecoj.12188, https://doi.org/10.1111/ecoj.12188.

[15] D. K. Foley, T. R. Michl, and D. Tavani, *Growth and Distribution*, Harvard University Press, Cambridge, MA and London, England, 2019, https://doi.org/doi:10.4159/9780674239395. Second Edition.

[16] G. Giraud and M. Grasselli, *Household debt: The missing link between inequality and secular stagnation*, Journal of Economic Behavior and Organization, 183 (2021), pp. 901–927, https://doi.org/10.1016/j.jebo.2019.03.002.

[17] G. Giraud and Z. Weiye, *Endogenous growth with collateral and default*, EJP WP, 2 (2023). Working paper.

[18] W. Godley and M. Lavoie, *Monetary Economics: An Integrated Approach to Credit, Money, Income, Production and Wealth*, Palgrave Macmillan, London, UK, 2012, https://doi.org/10.1007/978-1-137-08599-3.

[19] R. M. Goodwin, *A Growth Cycle*, Palgrave Macmillan UK, London, UK, 1982, pp. 165–170, https://doi.org/10.1007/978-1-349-05504-3_12.

[20] H. S. Gordon, *The economic theory of a common-property resource: The fishery*, Journal of Political Economy, 62 (1954), pp. 124–142. https://www.jstor.org/stable/1825571.

[21] M. Grasselli and A. Huu, *Inflation and Speculation in a Dynamic Macroeconomic Model*, Journal of Risk and Financial Management, 8 (2015), pp. 285–310, https://doi.org/10.3390/jrfm8030285.

[22] M. R. Grasselli and B. Costa Lima, *An analysis of the Keen model for credit expansion, asset price bubbles and financial fragility*, Mathematics and Financial Economics, 6 (2012), pp. 191–210, https://doi.org/10.1007/s11579-012-0071-8.

[23] M. R. Grasselli and A. Maheshwari, *Testing a Goodwin model with general capital accumulation rate*, Metroeconomica, 69 (2018), pp. 619–643, https://doi.org/10.1111/meca.12204.

[24] M. R. Grasselli and A. Nguyen-Huu, *Inventory growth cycles with debt-financed investment*, Structural Change and Economic Dynamics, 44 (2018), pp. 1–13, https://doi.org/10.1016/j.strueco.2018.01.003.

[25] M. C. Hänsel, M. A. Drupp, D. J. A. Johansson, F. Nesje, C. Azar, M. C. Freeman, B. Groom,

AND T. STERNER, *Climate economics support for the UN climate targets*, Nature Climate Change, 10 (2020), pp. 781–789, https://doi.org/10.1038/s41558-020-0833-x, https://www.nature.com/articles/s41558-020-0833-x.

[26] L. HARDT AND D. W. O'NEILL, *Ecological Macroeconomic Models: Assessing Current Developments*, Ecological Economics, 134 (2017), pp. 198–211, https://doi.org/https://doi.org/10.1016/j.ecolecon.2016.12.027.

[27] E. HERBERT, A. LOUIS-NAPOLÉON, C. GOUPIL, AND G. GIRAUD, *Macroeconomic dynamics in a finite world: the thermodynamic potential approach*. Working paper, 2022, https://doi.org/10.48550/arXiv.2204.02038.

[28] J. HERMAN AND W. USHER, *SALib: An open-source python library for sensitivity analysis*, The Journal of Open Source Software, 2 (2017), https://doi.org/10.21105/joss.00097, https://doi.org/10.21105/joss.00097.

[29] S. IDEE, *Sensitivity analysis module for the idee model*. https://github.com/chevaldemetal/sa_idee_module, 2025. Accessed: 2025-02-12.

[30] IPCC, *Summary for Policymakers*, in Climate Change 2021: The Physical Science Basis, V. Masson-Delmotte, P. Zhai, A. Pirani, S. Connors, C. Péan, S. Berger, N. Caud, Y. Chen, L. Goldfarb, M. Gomis, M. Huang, K. Leitzell, E. Lonnoy, J. Matthews, T. Maycock, T. Waterfield, O. Yelekçi, R. Yu, and B. Zhou, eds., Contribution of Working Group I to the Sixth Assessment Report of the Intergovernmental Panel on Climate Change, Cambridge University Press., Cambridge, UK, 2021, pp. 3–31, https://www.ipcc.ch/report/ar6/wg1/chapter/summary-for-policymakers/.

[31] IPCC, *Summary for Policymakers*, in Climate Change 2022: Impacts, Adaptation, and Vulnerability. Contribution of Working Group II to the Sixth Assessment Report of the Intergovernmental Panel on Climate Change, H. O. Pörtner, D. C. Roberts, M. Tignor, E. S. Poloczanska, K. Mintenbeck, A. Alegría, M. Craig, S. Langsdorf, S. Löschke, V. Möller, A. Okem, and B. Rama, eds., Cambridge University Press, Cambridge, UK, jun 2022, pp. 3–33, https://doi.org/10.1017/9781009325844.001.

[32] T. IWANAGA, W. USHER, AND J. HERMAN, *Toward SALib 2.0: Advancing the accessibility and interpretability of global sensitivity analyses*, Socio-Environmental Systems Modelling, 4 (2022), p. 18155, https://doi.org/10.18174/sesmo.18155, https://sesmo.org/article/view/18155.

[33] P. JACQUES, L. DELANNOY, B. ANDRIEU, D. YILMAZ, H. JEANMART, AND A. GODIN, *Assessing the economic consequences of an energy transition through a biophysical stock-flow consistent model*, Ecological Economics, 209 (2023), p. 107832, https://doi.org/10.1016/j.ecolecon.2023.107832.

[34] S. KEEN, *Finance and Economic Breakdown: Modeling Minsky's "Financial Instability Hypothesis"*, Journal of Post Keynesian Economics, 17 (1995), pp. 607–635, https://doi.org/10.1080/01603477.1995.11490053, http://www.tandfonline.com/doi/full/10.1080/01603477.1995.11490053.

[35] G. LI, H. RABITZ, P. E. YELVINGTON, O. O. OLUWOLE, F. BACON, C. E. KOLB, AND J. SCHOENDORF, *Global Sensitivity Analysis for Systems with Independent and/or Correlated Inputs*, The Journal of Physical Chemistry A, 114 (2010), pp. 6022–6032, https://doi.org/10.1021/jp9096919.

[36] N. G. MANKIW, *Principles of economics*, Cengage Learning, Boston, USA, 2020.

[37] H. A. MARTIN, A. QUIQUET, T. NICOLAS, G. GIRAUD, S. CHARBIT, AND D. M. ROCHE, *Climate-induced economic damages can lead to private-debt tipping points*. Working paper, 2024, https://hal.science/hal-04224077.

[38] M. D. MORRIS, *Factorial Sampling Plans for Preliminary Computational Experiments*, Technometrics, 33 (1991), pp. 161–174, https://doi.org/10.1080/00401706.1991.10484804.

[39] W. NORDHAUS, *Evolution of modeling of the economics of global warming: changes in the DICE model, 1992–2017*, Climatic Change, 148 (2018), pp. 623–640, https://doi.org/10.1007/s10584-018-2218-y.

[40] F. PIANOSI AND T. WAGENER, *A simple and efficient method for global sensitivity analysis based on cumulative distribution functions*, Environmental Modelling & Software, 67 (2015), pp. 1–11, https://doi.org/10.1016/j.envsoft.2015.01.004.

[41] A. QUIQUET, D. M. ROCHE, C. DUMAS, AND D. PAILLARD, *Online dynamical downscaling of temperature and precipitation within the iLOVECLIM model (version 1.1)*, Geoscientific Model Development, 11 (2018), pp. 453–466, https://doi.org/10.5194/gmd-11-453-2018, https://gmd.copernicus.org/articles/11/453/2018/.

[42] SALIB, *Sensitivity Analysis Library in Python*. https://salib.readthedocs.io/en/latest/index.html, 2024. Accessed: 2025-02-12.

[43] A. Saltelli, *Making best use of model evaluations to compute sensitivity indices*, Computer Physics Communications, 145 (2002), pp. 280–297, https://doi.org/10.1016/S0010-4655(02)00280-1.

[44] A. Saltelli, P. Annoni, I. Azzini, F. Campolongo, M. Ratto, and S. Tarantola, *Variance based sensitivity analysis of model output. Design and estimator for the total sensitivity index*, Computer Physics Communications, 181 (2010), pp. 259–270, https://doi.org/10.1016/j.cpc.2009.09.018.

[45] B. M. Sanderson and B. C. O'Neill, *Assessing the costs of historical inaction on climate change*, Scientific Reports, 10 (2020), p. 9173, https://doi.org/10.1038/s41598-020-66275-4.

[46] I. Sobol, *Global sensitivity indices for nonlinear mathematical models and their Monte Carlo estimates*, Mathematics and Computers in Simulation, 55 (2001), pp. 271–280, https://doi.org/10.1016/S0378-4754(00)00270-6.

[47] I. Sobol and S. Kucherenko, *Derivative based global sensitivity measures and their link with global sensitivity indices*, Mathematics and Computers in Simulation, 79 (2009), pp. 3009–3017, https://doi.org/10.1016/j.matcom.2009.01.023.

[48] V. Spaiser, S. Juhola, S. M. Constantino, W. Guo, T. Watson, J. Sillmann, A. Craparo, A. Basel, J. T. Bruun, K. Krishnamurthy, J. Scheffran, P. Pinho, U. T. Okpara, J. F. Donges, A. Bhowmik, T. Yasseri, R. Safra de Campos, G. S. Cumming, H. Chenet, F. Krampe, J. F. Abrams, J. G. Dyke, S. Rynders, Y. Aksenov, and B. M. Spears, *Negative social tipping dynamics resulting from and reinforcing earth system destabilization*, Earth System Dynamics, 15 (2024), pp. 1179–1206, https://doi.org/10.5194/esd-15-1179-2024.

[49] J. E. Stiglitz, N. Stern, M. Duan, Edenhofer, Ottmar, G. Giraud, G. M. Heal, E. L. la Rovere, A. Morris, E. Moyer, M. Pangestu, P. R. Shukla, Y. Sokona, and H. Winkler, *Report of the High-Level Commission on Carbon Prices*, tech. report, International Bank for Reconstruction and Development and International Development Association/The World Bank, 2017, https://doi.org/10.7916/d8-w2nc-4103.

[50] B. H. Strauss, P. M. Orton, K. Bittermann, M. K. Buchanan, D. M. Gilford, R. E. Kopp, S. Kulp, C. Massey, H. de Moel, and S. Vinogradov, *Economic damages from Hurricane Sandy attributable to sea level rise caused by anthropogenic climate change*, Nature Communications, 12 (2021), p. 2720, https://doi.org/10.1038/s41467-021-22838-1.

[51] S. Tarantola, D. Gatelli, and T. Mara, *Random balance designs for the estimation of first order global sensitivity indices*, Reliability Engineering & System Safety, 91 (2006), pp. 717–727, https://doi.org/10.1016/j.ress.2005.06.003.

[52] J. B. Taylor, *Discretion versus policy rules in practice*, Carnegie-Rochester Conference Series on Public Policy, 39 (1993), pp. 195–214, https://doi.org/10.1016/0167-2231(93)90009-L.

[53] F. van der Ploeg, *Classical Growth Cycles*, Metroeconomica, 37 (1985), pp. 221–230, https://doi.org/10.1111/j.1467-999X.1985.tb00412.x.

Appendix A. Tables.

Table 2
Full model variables and parameters

Symbol	Description	Value	Eq.
N	Global workforce	(variable)	(2.1)
δ_N	Growth rate of workforce	0.0305	(2.1)
$\bar{N}$	Maximum workforce	7.06	(2.1)
a	Labor productivity	(variable)	(2.2)
δ_a	Intercept of the linear function	0.01	(2.2)
γ_g	Slope of the linear function	0.5	(2.2)
$\delta_a^{\min}$	Maximum degrowth rate of productivity	-0.02	(2.2)
Y^0	Potential aggregated production	(variable)	(2.3)
ν	Capital-to-output ratio	3.0	(2.3)
Y	Real output	(variable)	(2.4)
g	Real growth rate	(variable)	(2.4)
δ_Y	Total fraction of "lost" production	(variable)	(2.4)
K	Capital	(variable)	(2.5)
δ_K	Capital depreciation rate	(variable)	(2.5)
δ	Constant standard depreciation rate	0.04	(2.5)
Π	Profit before dividends	(variable)	(2.6)
π	Profit ratio	(variable)	(2.6)
π_K	Return rate on capital	(variable)	(2.6)
W	Wage bill	(variable)	(2.6)
T_f	Carbon tax	(variable)	(2.6)
I	Real investment	(variable)	(2.7)
κ_0	Intercept of the linear investment function	0.0397	(2.7)
κ_1	Slope of the linear investment function	0.719	(2.7)
$\kappa_{\min}$	Minimum of the investment function	0.0	(2.7)
$\kappa_{\max}$	Maximum of the investment function	0.3	(2.7)
ζ_I	Parameter of the investment function	0.25	(2.7)
d	Debt ratio	(variable)	(2.8)
Γ	Fraction of capital seized	(variable)	(2.9)
χ	Parameter in the function of the capital seized	0.0045	(2.9)
D	Nominal private debt	(variable)	(2.10)
Π_r	Retained earnings of firms	(variable)	(2.10)
γ_Γ	Debt forgiveness ratio	1.05	(2.10)
Δ_0	Intercept of the linear dividend function	0.0275	(2.10)
Δ_1	Slope of the linear dividend function	0.4729	(2.10)
$\Delta_{\min}$	Minimum of the dividend function	0	(2.10)
$\Delta_{\max}$	Maximum of the dividend function	0.3	(2.10)
w	Nominal wage *per-capita*	(variable)	(2.11)
ϕ_0	Intercept of the linear Philips curve	-0.292	(2.11)
ϕ_1	Slope of the linear Philips curve	0.469	(2.11)
γ_w	Parameter of the money illusion	0.5	(2.11)
ω	Wage share	(variable)	(2.12)
λ	Employment rate	(variable)	(2.12)
p	Price of goods	(variable)	(2.13)
i	Inflation rate	(variable)	(2.13)
η	Relaxation parameter of inflation	0.2	(2.13)
μ	Price markup	(variable)	(2.13)
μ_0	Constant term in the price markup	1.7	(2.13)
r	Short-term interest rate	(variable)	(2.14)
r_{CB}	Central Bank interest rate	(variable)	(2.14)
$i^\star$	Inflation rate targeted by the monetary policy	0.02	(2.14)
$r^\star$	Long-term interest rate target	0.02	(2.14)
ψ	Reactivity of the monetary policy	0.5	(2.14)
η_r	Relaxation parameter of the interest rate	0.333	(2.14)
ΔT	Mean air temperature elevation	(variable)	(2.15)
Dam	Fraction of capital lost due to climate	(variable)	(2.15)
D_K	Fraction of capital lost due to climate	(variable)	(2.15)
D_Y	Fraction of production lost due to climate	(variable)	(2.15)
Υ_1	Parameter of the damage function	0	(2.15)
Υ_2	Parameter of the damage function	0.00236	(2.15)
Υ_3	Parameter of the damage function	0.0000819	(2.15)
ζ_3	Parameter of the damage function	6.75	(2.15)
f_K	Fraction of damages on capital	0.333	(2.15)
E_{ind}	Emissions due to economic activities	(variable)	(2.16)
σ	Carbon-emission intensity	(variable)	(2.17)
δ_σ	Parameter in the carbon-emission intensity	-0.014936	(2.17)
γ_σ	Abatement coefficient in the carbon-emission intensity	0.2	(2.17)
A	Abatement ratio	(variable)	(2.18)
p_{BS}	Price of the back-stop technology	(variable)	(2.18)
$\delta_{p_{BS}}$	Growth rate of the back-stop technology price	-0.0026	(2.18)
$\gamma_{p_{BS}}$	Abatement Coefficient in the p_{BS} equation	0.5	(2.18)
n	Emission reduction fraction	(variable)	(2.19)
s_a	Share of public subsidies	0.5 (moderate)	(2.19)
θ	Parameter of the abatement function	3.4	(2.19)
p_C	Carbon price	(variable)	(2.20)
a_{p_C}	Carbon price parameter	-0.004	(2.20)
b_{p_C}	Carbon price parameter	1.749	(2.20)

Table 3
Range of parameters

Group	Symbol	Lower bound	Upper bound	Default value	Eq.
Capital K	δ	0.035	0.045	0.040	(2.5)
Capital K	ν	2.61	3.39	3.00	(2.3)
Inflation i	η	0.17	0.23	0.20	(2.7)
Inflation i	μ_0	1.666	1.734	1.700	(2.7)
Investment I	κ_0	0.029775	0.049625	0.039700	(2.7)
Investment I	κ_1	0.53925	0.89875	0.719000	(2.7)
Productivity p	δ_a	0.0075	0.0125	0.0100	(2.2)
Productivity p	γ_g	0.375	0.625	0.500	(2.2)
Dividends D	Δ_0	0.020625	0.034375	0.027500	(2.10)
Dividends D	Δ_1	0.354675	0.591125	0.472900	(2.10)
Population N	δ_N	0.02	0.08	0.05	(2.1)
Population N	$\bar{N}$	4.662	5.418	5.040	(2.1)
Phillips P	ϕ_0	-0.293752	-0.290248	-0.292000	(2.11)
Phillips P	ϕ_1	0.452585	0.485415	0.469000	(2.11)
Phillips P	γ_w	0.45	0.55	0.50	(2.11)
Interest rate r	ψ	0.3	0.7	0.5	(2.14)
Interest rate r	i^*	0.012	0.028	0.020	(2.14)
Interest rate r	r^*	0.012	0.028	0.020	(2.14)
Interest rate r	η_r	0.256	0.476	0.333	(2.14)
Debt forgiveness	γ_Γ	1.05	1.05	1.05	(2.10)

Table 4
Initial values of the economic model (2015)

Symbol	Description	Value	Units	Eq.
N	Global workforce	4.83	workers bil.	(2.1)
Y	Aggregated production	58.7	2015 USD tril.	(2.4)
d	Private debt ratio	1.53		(2.8)
λ	Employment rate	0.675		(2.12)
ω	Wage share	0.578		(2.12)
i	Inflation	0.018		(2.13)
p	Normalized price	1		(2.13)
r	Interest rate	0.01		(2.14)
ΔT	Global annual mean air surface temperature anomaly	1.07	°C	(2.15)
E_{ind}	Emissions due to economic activities	51.8	$GtCO_2e$	(2.16)
p_{BS}	Price of the backstop technology	1500	2015 USD/tCO_2e	(2.18)
n	Emission reduction ratio	0.03		(2.19)